32

A study of copper diffusion through Pd_2Si thin films

by

Dieter Rudi Geduld

Thesis presented for the degree of

Master of Science

in the Department of Physics

Faculty of Science

University of Cape Town

February 1997

Abstract

It is now generally recognized that unless an alternative for aluminium is found the resistivity of the metal interconnects will soon limit device performance. Copper, with its low resistivity and greater resistance to electromigration is one of the obvious substitutes. However, before aluminium can be replaced by copper, a careful study of the reactivity of copper with metal-silicides used in devices needs to be carried out. This study involves a *dynamic* **RBS** investigation of the reaction of copper with Pd_2Si films grown on Si<100> and Si<111> substrates. It was found that copper diffused through the Pd_2Si layer and reacted with the single crystal silicon substrate at relatively low temperatures. The onset temperature observed for copper diffusion was found to differ for Pd_2Si films grown on the two different substrate orientations, Si<100> and Si<111>. Measurements of the activation energies for Cu-silicide growth on Pd_2Si/Si<100> and Pd_2Si/Si<111> were also made.

Acknowledgements

I express my appreciation and gratitude to:

Professor Craig Comrie who supervised this work, for his tireless assistance, patience, wisdom and guidance throughout the duration of this project;

Dr. R. Pretorius, Van de Graaff Group, National Accelertor, Faure, for the interest he maintained throughout this study and the endless motivation to do well;

C.C. Theron for making this endeavour successful with regard to the experimental work, for the guidance in understanding *dynamic* **RBS**, the many enlightening and fruitfull discussions, and of course for preparing the novel 3-D plots;

Dr. R.Y. Naidoo, Dr. T.K. Marais and Dr. C.L. Churms for their assistance during the running of experiments, and the many helpful and fruitful discussions;

The staff at the Van de Graaff, Mrs. G. Stone, Mr. K. Springhorn, Messrs. C.J. Cloete, W.J. Cloete and S. Hendricks for their help enthusiasm and loads of encouragement;

Dr. Saalih Allie for his invaluable assistance in understanding the inner workings of *Scientific Workplace (SW20)*;

My parents, who unselfishly gave me all the guidance, strength and motivation to be the person I am today, thank you. My sisters, for putting in my lunch and really making the effort to accomodate me during the period of this project;

Renée, who undoubtedly has made immense sacrifices for me. For that, I love her.

Contents

List of Figures

List of Tables

Chapter 1

Introduction

We live in a period of rapid advancement in microelectronics technology. Present day microelectronic devices are no longer just diodes or transistors but are either large scale integrated circuits or special purpose components. The application of thin film technology in the electronics industry is based on the knowledge of the physical processes occurring in the deposition, operation and utilization of thin film structures. Critical aspects of modern thin film technology are the growth of epitaxial layers, interdiffusion and reactions that occur in thermal processing of the thin film structures. Advances in thin film and layered structure technology have been pivotal in the evolution of integrated circuits and opto-electronics. This chapter deals with the importance of copper as a substitute for aluminium as well as the importance of silicides. There will be discussions on silicides, silicide formation, epitaxial silicides, as well as reaction kinetics and kinetic parameters and measurements used to do the data analysis.

The fundamental building blocks of thin film technology are semiconductor materials. These materials are distinguished by having their specific electrical conductivity somewhere between that of good conductors ($10^6\ \Omega^{-1}\text{cm}^{-1}$) and that of good insulators ($10^{-5}\ \Omega^{-1}\text{cm}^{-1}$). Among these materials, by far the most important in microelectronic technology is silicon. The vast improvements in the speed and versatility of silicon electronics have mostly resulted from the miniaturization of circuitry. As device dimensions approach the submicron regime, reliability becomes an important issue. The resulting demands on interconnect technologies necessitate the exploitation of all de-

velopment avenues; i.e. design, materials and manufacturing. Multilevel metallization has also become an area of intense research [Mi94, St95, Fu95, Sh95]. Metallization generally requires good conductivity, resistance to electromigration, controllable contact performance, corrosion resistance, adherence, thermal stability, bondability and economic feasibility.

Aluminium and its alloys have been a commonly used metallization material. It does however, suffer from major limitations such as electromigration and stress-voiding induced open circuit failure [Li93]. When aluminium is deposited on the silicide, stability is lost during thermal processing. The aluminium reacts with the silicide and degrades its electrical properties. Copper is a candidate for on chip metallization because of its low bulk electrical resistivity and its resistance to electromigration. Copper interconnect technology has been widely studied in the past [Ka93, Mu93, Li94, Ha94, Ge94, Mi94]. With its low resistivity of $1.67\mu\Omega$ cm compared with $2.66\mu\Omega$ cm for aluminium, it is capable of carrying higher current densities with smaller line widths. Along with copper, gold and silver also have a high conductivity compared with aluminium and tungsten. However, all three of these metals form deep levels in the band gap of silicon, so it is difficult to use them as local interconnects in contact with silicon. The performance advantages and processing problems for these metals are listed in Table 1.1.

Table 1.1: *Comparison of materials properties and process problems among five metals. The line width used for electromigration resistance measurements was 0.5 μm. From Li et al. [Li94].*

	Al	W	Au	Ag	Cu
Resistivity ($\mu\Omega$ cm)	2.66	5.65	2.35	1.59	1.67
Electromigration resistance	low	very high	very high	very low	high
Corrosion resistance in air	high	high	very high	low	low
CVD processing	$\surd$	$\surd$	?	?	$\surd$
Dry etch processing at low temp.	$\surd$	$\surd$	?	?	?

As indicated in the Table 1.1 aluminium is highly corrosion resistant. This is of course only true once the protective oxide layer has grown because aluminium oxidizes very fast. Various obstacles to implementing copper interconnects in actual silicon devices include non-protective oxide formation and poor adhesion to silicon dioxide. The relatively low interfacial reaction temperatures between copper and most contact materials, particularly silicon, also causes a serious stability problem in copper based metallization.

1.1 Silicides

The motivation for studying silicide formation is due to the requirements placed on the performance of integrated circuits. Silicide films are employed in two ways in integrated silicon devices; (i) as Schottky barriers and (ii) ohmic contacts. In contacts, it is the ability of many transition metal films to form a uniform stable silicide layer with the silicon substrate by a solid phase reaction that has led to their use.

1.1.1 Silicide Formation

A silicide is formed by the reaction between a metallic thin film in contact with silicon [Ma90]. If a metal film is deposited on the silicon substrate then the silicon in the subsequent metal-silicon reaction is drawn from the silicon substrate. Whereas, if the silicide film is deposited on an inert substrate, for example SiO_2, then both the silicon and the metal have to be laid down and their ratio has to conform to the desired stoichiometry.

It is important to note that the sample must be subjected to a treatment e.g. conventional furnace annealing, laser annealing or ion beam annealing, that will promote the reaction between the metal film and the substrate. As shown schematically in Fig. 1.1, the silicide may grow by diffusion of metal or silicon across it. There are numerous examples of metal-silicon compounds or silicides, but Pd_2Si, NiSi, PtSi and $CoSi_2$ are of good examples of silicides that are important in the microelectronics industry. Growth kinetics for metal-rich silicides typically follow a parabolic law and the

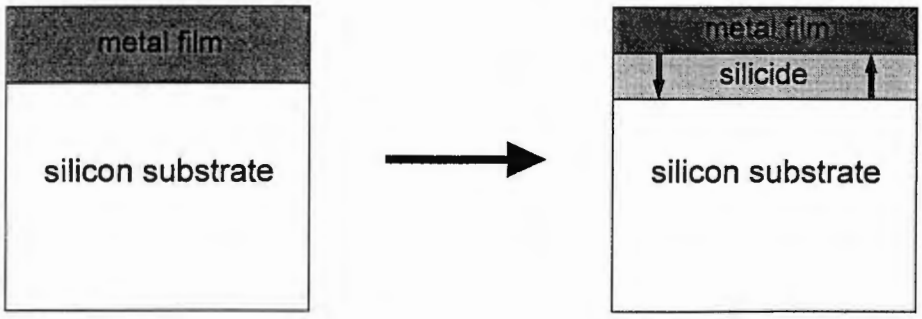

Figure 1-1: *Formation of a metal silicide. As indicated by the small arrows, either the metal atoms or the silicon atoms could be diffusing species.*

formation temperatures begin at around 200°C [Tu78].

Uniform and flat interfaces are usually required for electronic devices. These planar interfaces arise naturally during silicide formation. The vacuum evaporation of transition metals requires very high crucible temperatures and some of these metals tend to react rapidly with oxygen or carbon so that the reproducible deposition of clean layers can be instrumentally demanding. Good vacuum and contamination free interfaces are required during deposition. Impurities, hydrocarbon layers and oxides can all impede the metal-silicon reaction and lead to rough interfaces [Tu92].

1.1.2 Epitaxial Silicides

It seems obvious that crystal orientation and the microstructure of the silicide may play an important role in the fabrication of almost all semiconductor devices. When metal films are deposited on single crystal substrates, the compound layers may show preferred orientation. An epitaxial relationship involves the growth of an overlayer whose major axes are orientated parallel to the major axis of the underlying substrate. A necessary condition for good epitaxial growth is the matching of the lattice parameters between the compound and the underlying single-crystal semiconductor substrate.

Table 1.2: *General properties of four silicides observed to grow epitaxially on silicon. Reproduced from Tung et al. [Tu82].*

Silicide	PtSi	Pd_2Si	$CoSi_2$	$NiSi_2$
Structure	Orthorhombic	Hexagonal	Cubic	Cubic
Lattice mismatch (%)	9.5	2.2	1.2	0.4
Formation temperature (°C)	300	100 - 700	550 - 1000	750 - 800
Substrate	(111)	(111)	(111) (100)	(111) (100)
Preferred orientation	< 100 >	< 001 >	< 111 > -	< 111> - < 100 >
Channeling χ_{min} (%)	19	15	12 - poor	5 - 12

Polycrystalline films of reasonable epitaxial quality can be grown on single crystal silicon substrates by conventional deposition and annealing techniques [Tu82]. The better known epitaxial silicides are displayed in Table 1.2.

The channeling referred to in Table 1.2 is a form of backscattering (**RBS**) analysis. The channeling effect arises because the rows or planes within the crystal lattice can 'steer' the projectile ions along these rows or planes. Aligning the incident beam along these planar directions within the lattice causes a large decrease in the yield of the backscattered ions. Conversely if the lattice periodicity is not continuous throughout the lattice, i.e. atoms occupying interstitial sites or voids are present then dechanneling occurs and hence the yield increases. Therefore the ratio of the yields (heights of the **RBS** spectra) of the aligned spectrum with respect to the unaligned or random spectrum indicates the epitaxial quality of the crystal. This ratio is represented by the symbol χ_{min}. It must be noted that the χ_{min} values presented in Table 1.2 are for silicides reacted under non-ultrahigh vacuum and conventional thermal annealing conditions. Under ultrahigh vacuum (UHV) conditions χ_{min} values of less than 5% can be achieved. Other factors that influence epitaxial growth include substrate surface cleanliness, source purity, substrate heating, deposition rate and annealing conditions [Ch86].

Palladium silicide (Pd_2Si) is of particular interest in the present study. The palladium silicide has a hexagonal (Fe_2P) crystal structure with unit cell dimensions of

a = 6.496 Å and c = 3.433 Å [Ni83]. Pd_2Si grows with the c axis perpendicular to all substrates, irrespective of the substrate orientation. Since Pd_2Si has a hexagonal crystal structure it is possible to match the hexagonal ab plane of the Pd_2Si with the hexagonal Si<111> surface. Clearly this is not possible with the Si<100> substrate because it has a 4-fold symmetry. Pd_2Si is therefore observed only to grow epitaxially on single crystal silicon with orientation <111> [Tu82, Is80, Ni83]. The epitaxial ab axis alignment with Si<111> will result in the formation of low angle grain boundaries in the polycrystalline Pd_2Si structure. These grain boundaries are termed low if the angular mismatch between the crystal grains is small. Namely if the ab axes of two corresponding crystal grains, a^1b^1 and a^2b^2, are relatively well aligned with one another,as indicated in Fig.1.2. For reasons explained above the angle boundaries would be larger for Si<100>. Hence it is possible to grow Pd_2Si with low or larger angle grain boundaries by growing the silicide on different orientations of the silicon substrate.

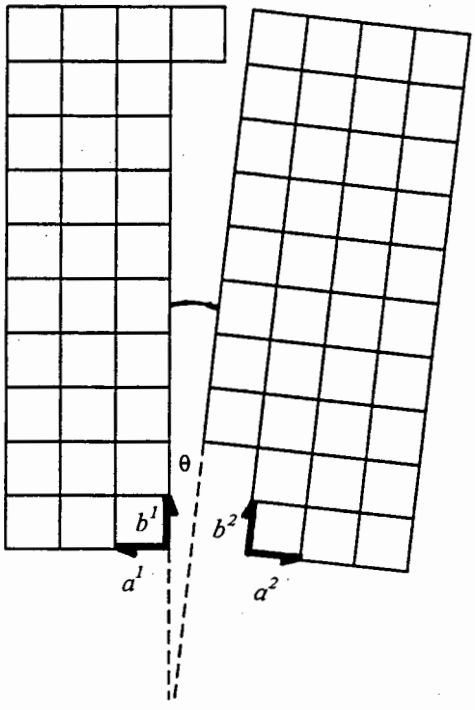

Figure 1-2: *A simple grain boundary. The plane of the figure is parallel to a cube face. The two grains have a common cubic axis and an angular difference in orientation θ. Reproduced from Mayer and Lau [Ma90].*

1.1.3 Reaction Kinetics

Solid-state reactions for silicide formation under steady-state conditions can be divided into two general categories; (i) systems that exhibit laterally uniform growth with well defined kinetics and temperature dependence, and (ii) systems that show laterally non-uniform growth and exhibit a critical temperature dependence [Ma90]. In the first category of silicide formation, the reaction takes place in a uniform layer by layer manner, over a wide range of temperatures. In the second category growth only takes place after a critical temperature has been reached and then within a narrow temperature range, typically 10°C to 30°C.

Consider the silicide formation reaction:

$$2\text{M (metal)} + \text{Si} \longrightarrow \text{M}_2\text{Si} \tag{1.1}$$

For this reaction to take place it must be thermodynamically possible. This condition is met by requiring the change in free energy, ($\triangle G$), to be negative. Though in general the kinetics of the reaction depend on atomic mobility, we have to consider two important issues in this regard, i.e. nucleation and growth. When a new phase is formed, M_2Si in this reaction, it is necessary for the reacting elements to get together near the interface and form a nucleus of the appropriate composition and structure. In this way a new surface encompassing the nucleus is also created, which may offer resistance to the nucleation, accompanied by an increase in the total surface energy. We know however that there is a gain in free energy required for the reaction to occur and this free energy is proportional to the volume of the newly formed phase. Therefore the total change in free energy at a given temperature T may be written as [Ma90]

$$\triangle G = \frac{4}{3}\pi r^3 \triangle G_v + 4\pi r^2 \triangle \sigma, \tag{1.2}$$

where $\triangle G_v$ is the change in free energy per unit volume and $\triangle \sigma$ is the change in surface energy per unit area.

After nucleation, any increase in the volume of the silicide is due to growth of the nuclei, which only requires atomic mobility. If the growth rate is faster than the

nucleation rate then the silicide formation is said to be nucleation controlled. If the nucleation rate is faster than the growth rate the silicide formation is growth controlled. The steady state silicide growth can be dealt with analogously to the oxidation reaction model proposed by Deal and Grove (1965) [De65]. The model is discussed in depth by Mayer and Lau [Ma90]. A schematic diagram of the model is shown in Fig. 1.2. C_o is the concentration of the metal atoms at the metal-silicide interface, C_i is the concentration of metal atoms at the silicide-silicon interface, and x_o the thickness of the silicide layer at time t.

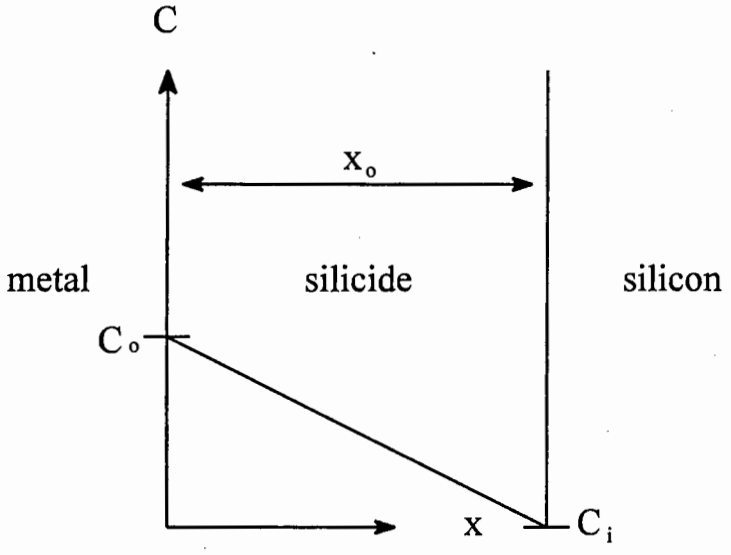

Figure 1-3: *Model of the thermal growth of a silicide phase (M_2Si) under steady-state annealing conditions. The metal atoms are assumed to be the main diffusing species [Th94].*

Assuming that the metal atoms M are the diffusing species then the diffusional flux F_1 of M across the already present silicide layer is given by

$$F_1 = \frac{D[C_o - C_i]}{x_o} \tag{1.3}$$

where D is the diffusivity. The flux to incorporate the reacting species into the silicon is given by

$$F_2 = k_s C_i \tag{1.4}$$

where k_s is the chemical reaction rate constant for silicide formation at the silicide-

silicon interface. When a steady state condition is established all the fluxes are equal and we have

$$C_i = \frac{C_o}{1 + \frac{k_s x_o}{D}}. \tag{1.5}$$

The flux $F = F_1 = F_2$, is then given by,

$$F = \frac{DC_o k_s}{D + k_s x_o} \tag{1.6}$$

and thus the rate at which the silicide grows is

$$\frac{dx_o}{dt} = \frac{F}{N_D} = \frac{DC_o k_s}{N_D} \frac{1}{D + k_s x_o}. \tag{1.7}$$

In Eq. (1.7) N_D denotes the number of diffusing (metal) atoms incorporated into a unit volume of silicide.

If the interfacial reaction is the rate limiting step, the reaction rate is less than the rate of atoms arriving at depth $x(t)$, then $D/x(t) \geq k_s$, $dx/dt = C_o k_s / N_D$ or $x = (C_o k_s / N_D)t$. The silicide thickness therefore increases linearly with time. If diffusion is the rate limiting step, the rate of atoms arriving at depth $x(t)$ is less than the reaction rate, then $D/x(t) \leq k_s$, $dx/dt = (DC_o/N_D)(1/x)$ or $x = (2DC_o t/N_D)^{\frac{1}{2}}$. The silicide thickness therefore increases with the square root of time. The growth of near noble metal silicides (e.g. Ni_2Si, NiSi, Pt_2Si, PtSi, Pd_2Si) follows a $t^{\frac{1}{2}}$ relationship while some transition-metal silicides (e.g. $CrSi_2$) follow a linear dependence. Examples of nucleation controlled silicide formation include the formation of $HfSi_2$ from HfSi, $IrSi_3$ from Ir_4Si_7, $NiSi_2$ from NiSi and certain rare earth metal silicides such as $ErSi_{1.7}$ [Ma90].

1.2 Kinetic Parameters and Measurements

In order to analyze or understand the kinetic processes and parameters which govern the reaction we need to determine the course of events as a function of time and temperature and to develop a method of observing this in a controlled manner. The basic parameters of interest are; atomic diffusivities, surface and interface energies, interfacial reaction constants, and enthalpy (heat) of formation or activation energy.

To relate these parameters to a reaction, the activation barrier to a reaction consists of surface energies spent in nucleation and of the activation energy of atomic diffusion. To overcome the barrier, heat is supplied. The reaction produces a product because of the gain in formation energy of the product, which is the driving force of the reaction. Under a driving force, the reaction rate can be diffusion-controlled or interfacial reaction-controlled. The following mathematical characterization of kinetic parameters and measurements is well covered by Tu, Mayer and Feldman [Tu92].

When the dependence of the layer thickness (x) on time (t) at a fixed temperature is measured, a plot of x vs t and x vs $t^{\frac{1}{2}}$ is done to determine whether the rate is interfacial reaction or diffusion-controlled. The relationship between x and t for a diffusion controlled reaction is usually taken to be

$$x^2 = 4Dt \tag{1.8}$$

where $D = D_o e^{-\frac{\triangle H}{kT}}$ and $\triangle H$ is the activation enthalpy which controls the reactions. For the interfacial reaction controlled reaction, the relation

$$x = Kt \tag{1.9}$$

can be used where $K = K_o e^{-\frac{\triangle H}{kT}}$ and $\triangle H$ is the enthalpy.

If it is possible to make a quasi-continuous measurement of the thickness or growth as a function of temperature, then another possibility of analysis arises.

For a diffusion-controlled reaction with the growth of the intermetallic compound following layered mode of growth, the thickness of the layer can be written as

$$x^2 = \int_0^t 4Ddt = \int_{T_i}^{T_f} 4D\frac{dt}{dT}dT \tag{1.10}$$

where x is thickness of the compound formed, D is the interdiffusion coefficient in the compound, t the reaction time and dT/dt is a constant ramping rate. If $D = D_o e^{-\frac{\triangle H}{kT}}$ and $\triangle H$ are time independent, then Eq. (1.10) relationship can be integrated to obtain

$$x^2 = 4D_o \frac{dt}{dT} \frac{k}{\triangle H} (T_f^2 e^{-\frac{\triangle H}{kT_f}} - T_i^2 e^{-\frac{\triangle H}{kT_i}}) \tag{1.11}$$

If the T_i is significantly smaller than T_f then the second term in brackets is small in comparison to the first term, therefore the second term can be neglected. Therefore the thickness for diffusion controlled growth can be given by

$$x^2 = 4D_o \frac{dt}{dT} \frac{kT^2}{\triangle H} e^{-\frac{\triangle H}{kT}}. \tag{1.12}$$

If we linearize Eq. (1.12) by dividing both sides by T^2 and then taking the natural logarithm of both sides the following equation is then obtained,

$$\ln(\frac{x^2}{T^2}) = \ln(4D_o \frac{dt}{dT} \frac{k}{\triangle H}) - \frac{\triangle H}{kT}. \tag{1.13}$$

Hence the activation enthalpy $\triangle H$ can be determined from the slope of a plot of $\ln(x^2/T^2)$ versus $(1/T)$. Knowing $\triangle H$, then the only unknown that needs to be determined is the interdiffusion coefficient D_o, since all the other variables are dependent on the experimental setup.

For an interfacial reaction-controlled mechanism, the thickness can be written as

$$x = \int_0^t K dt = \int_{T_i}^{T_f} K \frac{dt}{dT} dT \tag{1.14}$$

where $K = K_o e^{-\frac{\triangle H}{kT}}$ is the interfacial reaction constant. By repeating the procedure as above the thickness can be written in the form

$$x = K_o \frac{dt}{dT} \frac{kT^2}{\triangle H} e^{-\frac{\triangle H}{kT}}. \tag{1.15}$$

Again by linearizing this equation into the form

$$\ln(\frac{x}{T^2}) = \ln(K_o \frac{dt}{dT} \frac{k}{\triangle H}) - \frac{\triangle H}{kT} \tag{1.16}$$

we see that a plot of $\ln(x/T^2)$ versus $(1/T)$ will provide us with the activation enthalpy

$\triangle H$, and finally the pre-exponential factor K_o.

So an obvious advantage of this method is that all the data required to determine the activation energy for example, can be acquired from one sample. Further advantages will be discussed in chapter 4.

1.3 Mechanisms of Diffusion

Vibrations of atoms about their equilibrium position in crystal structures is well known. If the thermal energy is increased sufficiently enough then these oscillations become violent enough to allow the atoms to change sites. This change of location from one site to another gives rise to diffusion in solids. Since diffusion in crystalline solids is of primary interest, the discussion that follows will deal with the mechanisms in the context of the crystalline environment. There are other possible mechanisms, but in general, diffusion takes place in semiconductors via one or a combination of the several mechanisms which will be discussed below.

1.3.1 Interstitial Mechanism

An impurity atom located between the host atoms diffuses by the interstitial mechanism if it passes from one interstitial site to the next vacant site without permanently displacing any of the host atoms. This is indicated in Fig. 1.3a. As the impurity atom jumps from one site to another its motion is inhibited by the host atoms. It is this distortion of the host atoms that constitutes a barrier to the motion of the interstitial atom. This situation implies a sort of energy barrier. The jump frequency is therefore determined by how often this barrier can be overcome.

It will be dominant in any non-metallic solid in which the diffusing interstitial atom does not distort the lattice too much. If however the diffusing interstitial atom is not much smaller than the lattice atoms then the distortion involved becomes too large and another diffusion mechanism becomes more likely.

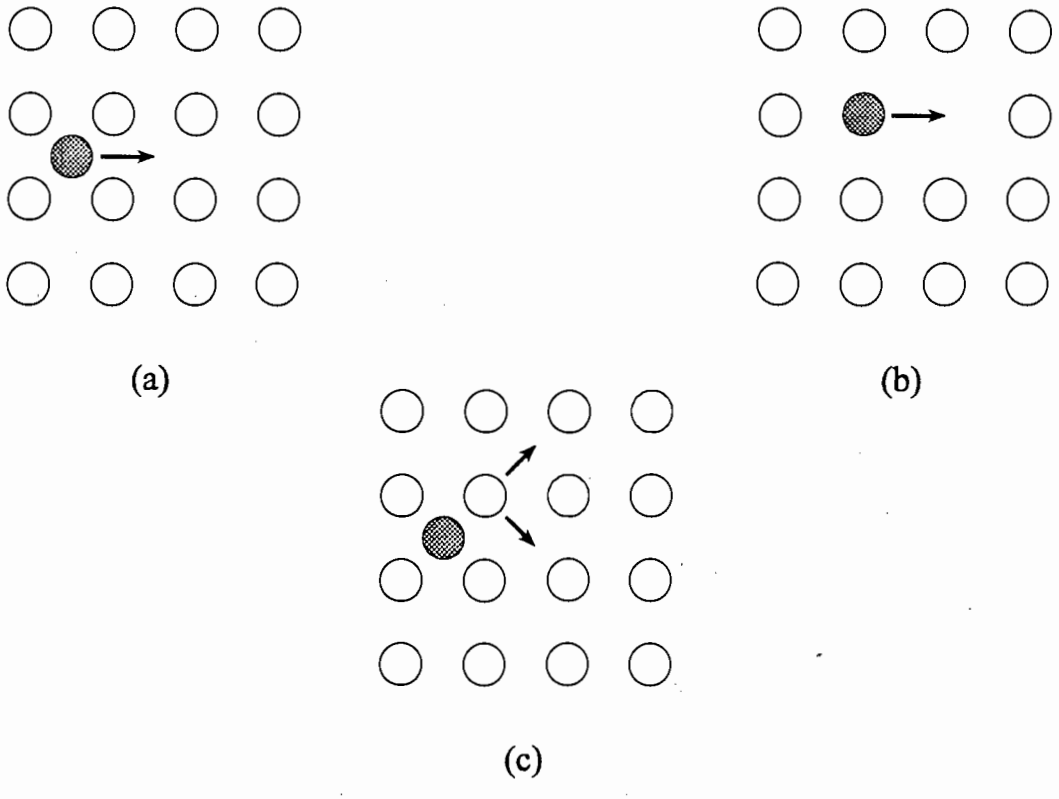

Figure 1-4: *Diffusion mechanisms; (a) Interstitial, (b) Vacancy and (c) Interstitialcy. Reproduced from Mayer and Lau [Ma90].*

1.3.2 Vacancy or Substitutional Mechanism

In crystalline solids not all lattice sites are occupied. These unoccupied sites are known as vacancies. An atom that jumps into a vacancy from an adjacent site is said to undergo diffusion via the vacancy or substitutional mechanism (Fig. 1.3b). In this case the probability of a jump into an adjacent site by the atom is dependent on two things. Firstly, the creation probability of a vacancy in the neighbouring lattice site and secondly the breaking of bonds and making of new bonds after the jump.

This method of diffusion is well established as the dominant mechanism in fcc metals and alloys [Bo88].

1.3.3 Interstitialcy and the Kick-Out Mechanism

Impurity atoms that are comparable in size to the lattice atoms produce large distortions if they diffuse via the interstitial mechanism. The jump frequency for these impurity atoms is therefore small. These atoms therefore have to diffuse via a different method that causes less distortion in the lattice. An atom is said to diffuse by the interstitialcy mechanism if it displaces one of the nearest host atoms into an interstitial site and then occupies the lattice site previously occupied by the host atom. This is shown in Fig. 1.3c. Because the distortion involved in this sort of displacement is minimal for reasons mentioned earlier, the probability of occurrence is therefore higher than for the interstitial diffusion mechanism.

The kick-out mechanism is similar to the interstitialcy mechanism. In this case a host atom that is diffusing interstitially around the lattice may encounter an impurity atom occupying a lattice site. The host atom may then push the substitutional impurity atom into an adjacent interstitial site. Subsequently the impurity atom may then diffuse interstitially or occupy another host atom lattice site via the interstitialcy mechanism.

1.3.4 Grain Boundary Diffusion

A grain boundary may be defined as the interfacial transition region between two grains in a single-phase material, which are in contact with each other but differ in

crystallographic orientation [Ka95]. A simple grain boundary is depicted in Fig. 1.2.

The process of atomic transport of atoms along the grain boundaries in polycrystalline material is called grain boundary diffusion. In general the atomic transport or diffusion along these grain boundaries is orders of magnitude faster than diffusion in the bulk material [Tu92]. Also since these grain boundaries are highly disordered it could be suggested that they provide a more 'open' medium for diffusion compared with the mechanisms mentioned earlier. Thus it would be reasonable to expect that the activation energy for the diffusion process along the grain boundaries would in general have smaller values. There has been comparatively little research performed on this particular mechanism of diffusion and consequently the present knowledge on the subject is largely phenomenological.

Therefore what has been presented is a very brief and qualitative description of the diffusion mechanism. Theoretical treatments of grain boundary diffusion based on Fisher [Fi51] and Whipple [Wh54] are well presented in *Fundamentals of grain and interphase boundary diffusion* [Ka95] and *Electronic thin film science for electrical engineers and materials scientists* [Tu92].

The density of grain boundaries is particularly high in polycrystalline thin films, therefore grain boundary diffusion could be the most dominant transport mechanism in thin film structures at relatively low temperatures. Although there is no quantifiable, preferred diffusion in a general sense, the diffusion coefficients depend on the bulk material, the grain boundary orientation with respect to the diffusion source and on the form of the grain boundary itself [Ma84].

1.4 Scope of investigation

In this work the diffusion and reaction kinetics of copper deposited on Pd_2Si grown on Si<100> and Si<111> substrates was investigated. This system will be referred to in the text as $Cu/Pd_2Si/Si< >$. The experimental techniques used in the process of this investigation are described in chapter 2. The preliminary investigation, discussed in chapter 3, was concerned with the phase identification and behaviour of the system. The results of the dynamic Rutherford Backscattering Spectrometry investigation of

the $Cu/Pd_2Si/Si< >$ system is presented in chapter 4. Here an attempt will be made to determine the reaction kinetics of the system, i.e. the type of reaction mechanism and the activation energy associated with the growth mechanism. Finally a summary of all results and a conclusion is presented in chapter 5.

Chapter 2

Experimental

2.1 Sample Preparation

2.1.1 Wafer Preparation

Single crystal Si<100> and Si<111> samples were used as substrates to grow the silicides and multilayer thin films. The silicon wafers were either n or p doped with the resistivity varying between 1.5 and 2.5 Ω.cm. All substrates were sequentially degreased by ultrasonic cleaning in solutions of acetone and ethanol. After repeating this cleaning procedure the substrates were rinsed in a deionized water (H_2O) solution with a resistivity which is better than 10 MΩ.cm. To obtain high quality epitaxial films it was considered important to remove the native oxide layer on the silicon wafers. This was done by etching the substrate for 30 seconds in a dilute HF (hydrofluoric acid) solution and then drying the wafers under a stream of nitrogen gas prior to loading. The HF dip is reported to result in the removal of the native oxide layer (SiO_2) and leaving the surface reportedly terminated with hydrogen so that the rate of further oxidation is greatly retarded [Fe89]. The samples were then mounted on a substrate which could be heated and loaded into the high vacuum evaporation chamber.

2.1.2 Electron Beam Evaporation

The silicide films and intermediate buffer layers were prepared by using an electron-beam evaporation system in high vacuum. The target materials were placed in the three water-cooled crucibles. The crucibles were thoroughly cleaned between depositions of different target materials to prevent possible contamination of the deposit.

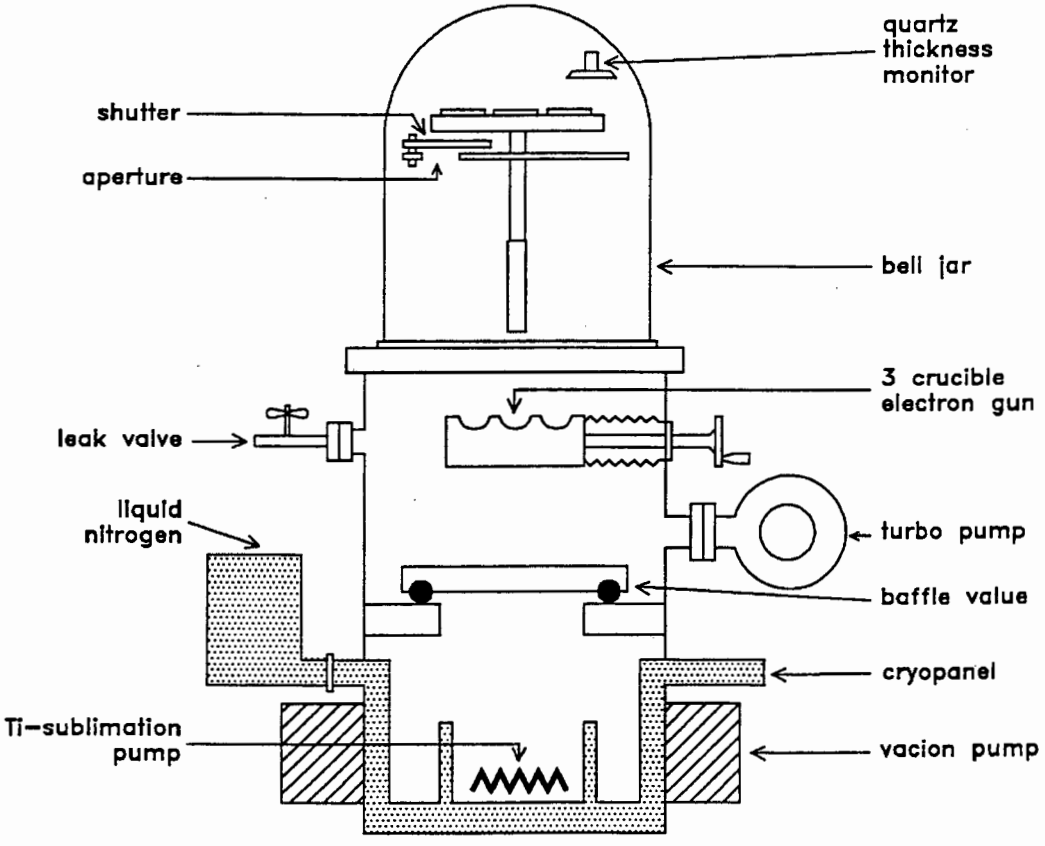

Figure 2-1: *A schematic diagram of the high vacuum evaporation chamber used to prepare the multilayer thin film structures.*

An oscillating quartz crystal monitor monitored the rate and thickness of the deposited material. The actual vacuum system consisted of an upper bell jar encased in a see through metal jacket and a lower pumping section which contained a VacIon pump, a Ti (titanium) sublimation pump and a liquid nitrogen cooled cryopanel. The important features of the vacuum evaporator chamber are shown in Fig. 2.1. The

upper bell jar was pumped by a turbomolecular pump which is capable of bringing the pressure to about 10^{-6} Torr. The lower section can achieve pressures of about 10^{-8} Torr. With both pumps together a low combined chamber pressure of 10^{-7} Torr could be achieved. These pressures were usually obtained by allowing the system to 'pump down' overnight prior to the actual evaporation. The two sections were isolated from each other by a baffle valve. This valve was closed when changing around samples and target materials so that a vacuum was maintained in the lower section at all times. Prior to the actual evaporation the target materials and the substrate heater were conditioned by pre-annealing, thereby outgassing possible contaminants in the target material and on the substrate heater.

2.1.3 The Heated Substrate

The substrate heater consisted of two aluminium plates that housed the two heater elements. Temperature was measured with a K-type thermocouple which was placed in a surface position in between the two heating elements. The thermocouple was connected to a temperature controller that monitors and controlled the temperature. In general the temperature of the substrate rises at a rate proportional to time during the heating stage. The heating rate was approximately linear, 15°C/min, from room temperature to 475°C. So it took about 30 minutes heat up from approximately 22°C to 475°C. When it was necessary to cool the substrate heater at the end of an anneal, a large aluminium block was lowered on to the substrate heater to act as a heat sink. During cooling, heat was lost at an exponential rate. An indication of this exponential heat loss was the fact that the heater took approximately 20 minutes to cool to about 370°C. And then about a further 60 minutes to achieve about 200°C. In all, the substrate heater took approximately four hours to cool from 475°C to about 70°C.

2.1.4 Vacuum Annealing

Some samples were further annealed in vacuum to enable solid-state reaction of multilayer thin films. Samples were loaded into a carrousel of a Lindberg tube furnace. The

carrousel system accommodated up to eight quartz boats, each capable of holding up to six samples. The quartz boats containing the samples were individually positioned in the centre of the heater elements of the furnace. The system vacuum was obtained by using a turbomolecular pump. A platinel Π thermocouple mounted directly above the quartz boat on the outer surface of the tube measured the temperature of the furnace. A Eurotherm temperature controller (microprocessor unit) was used to control the temperature. Heating of the samples was carried out at vacuum pressures in the low 10^{-7} Torr. A liquid nitrogen cold trap was used to reduce the water vapour levels inside the tube furnace, thereby increasing the probability of a good vacuum. The samples were allowed to cool down for approximately 30 minutes after annealing before the chamber was let up to atmospheric pressure by allowing in O_2 free nitrogen. Whenever possible the samples were stored under vacuum in the furnace to prevent possible oxidation and were only removed when ready for sample analysis.

2.2 Sample Characterization

2.2.1 Rutherford Backscattering Spectrometry

The use of ion backscattering for analysis of solids was first reported in 1913 by Geiger and Marsden [Ge13]. The technique has developed into a well established tool for near surface micro-analysis of materials. Rutherford Backscattering Spectrometry (**RBS**) is a fast and direct method for obtaining elemental depth profiles in solids [Ch78], and identification of elemental constituents. **RBS** was used to determine the thickness and extent of interaction of the deposited thin films. In the present investigation **RBS** was performed at the National Accelerator Centre, Faure using the Van de Graaff Accelerator to produce 2 MeV alpha particles.

The subject of **RBS** is very well covered in the book *Backscattering Spectrometry* by Chu, Mayer and Nicolet [Ch78]. Basically **RBS** entails directing a mono-energetic (E_o) and collimated beam of alpha particles on to the target, in this case the sample, and the elastically backscattered particles (E_1) are detected by a solid state detector as shown in Fig. 2.2. There are three basic concepts which are of importance in **RBS**,

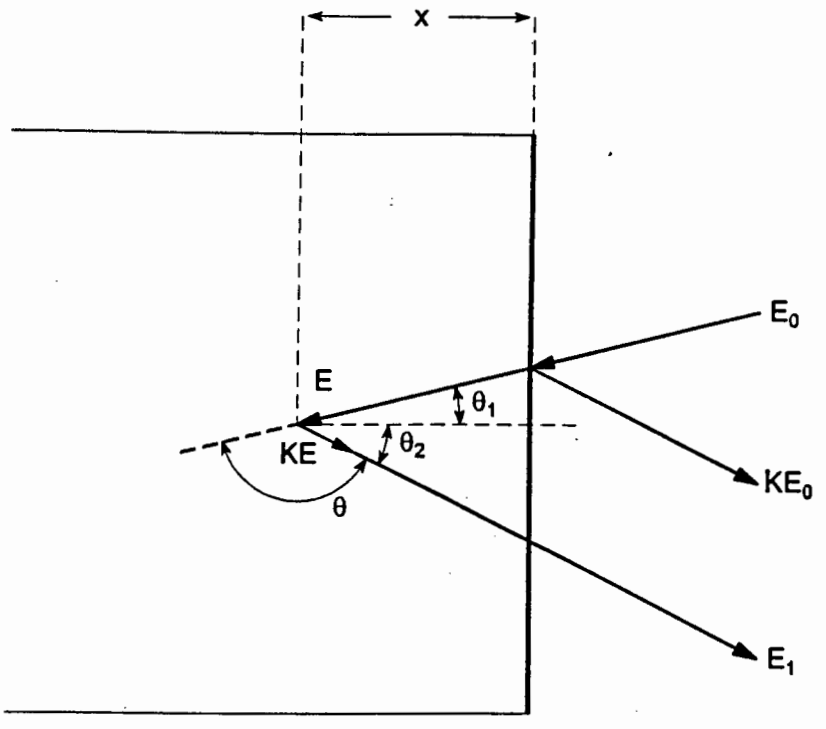

Figure 2-2: *Symbols used to describe the backscattering events in a sample. The incident beam, detector direction and the sample normal are all coplanar.*

each related to an analytical capability of the method;

1. The kinematic factor K, is defined as the ratio of the projectile energy after the collision E_1 to the incident projectile energy E_o.

$$K = \frac{E_1}{E_o} = \left[\frac{m\cos\theta + \left(M^2 - m^2\sin^2\theta\right)^{\frac{1}{2}}}{m+M}\right]^2 \tag{2.1}$$

   K is thus a function of M, the target atom mass. Therefore by measuring E_1, the mass of the target atom can be determined.

2. The differential scattering cross-section is given by

$$\frac{d\sigma}{d\Omega} = \left[\frac{zZe^2}{2E_o\sin^2\theta}\right]^2 \frac{\left[\cos\theta + \left\{1 - \left(\frac{m}{M}\sin\theta\right)^2\right\}^{\frac{1}{2}}\right]^2}{\left\{1 - \left(\frac{m}{M}\sin\theta\right)^2\right\}^{\frac{1}{2}}}, \tag{2.2}$$

   where $d\sigma/d\Omega$ is proportional to Z^2. Clearly the backscattering yield is large for high Z atoms. Therefore a quantitative analysis can be made of the atomic composition.

3. The difference in energy between a particle scattered from the surface, KE_o, and one that has been scattered at a depth x is given by

$$\triangle E = KE_o - E_1 = \left[\frac{K}{\cos\theta_1}\left(\frac{dE}{dx}\right)_{in} + \frac{1}{\cos\theta_2}\left(\frac{dE}{dx}\right)_{out}\right] \tag{2.3}$$

   where E_1 is a measured value associated with a particle scattered at a depth x (Fig. 2.2), and the energy loss per unit length, dE/dx, is averaged along the inward and outward journey. In the situation when the films under investigation are relatively small ($\leq$ 3000 Å) and the energies of the incident ions are large ($\sim$ 2MeV), the dependence of dE/dx on x is small. The energy $\triangle E$ is therefore approximately linearly related to the depth x. Eq. (2.3) can therefore be written as $\triangle E = [S]\,x$ where $[S]$ is the energy loss factor. A measurement of $\triangle E$ provides the ability of depth resolution.

In the present experimental setup the α-particles were directed onto the target contained in the vacuum chamber (pressure $\sim 10^{-5}$ torr) and the backscattered α's were detected with a silicon surface barrier detector. The detector angle was 170° from the incident beam which maximized the energy resolution of the system. The sample was mounted at a 10° tilt angle with respect to the beam. Since the beam spot is about 2 mm^2, the samples to be analyzed should have uniform lateral composition over at least such a dimension. Beam current was varied according to collimator size and the specific requirements for a particular film. Beam currents of up to 160 nA with total integrated charge 20 μC were used. The sample chamber was pumped by a turbomolecular pump to about 10^{-5} torr during analysis. These and other details can be seen in Fig. 2.3. The data were acquired via a live time data acquisition system and observed on a display monitor before being saved for further analysis. The beam current was measured by charge collected from the isolated chamber wall which was used as a Faraday cup.

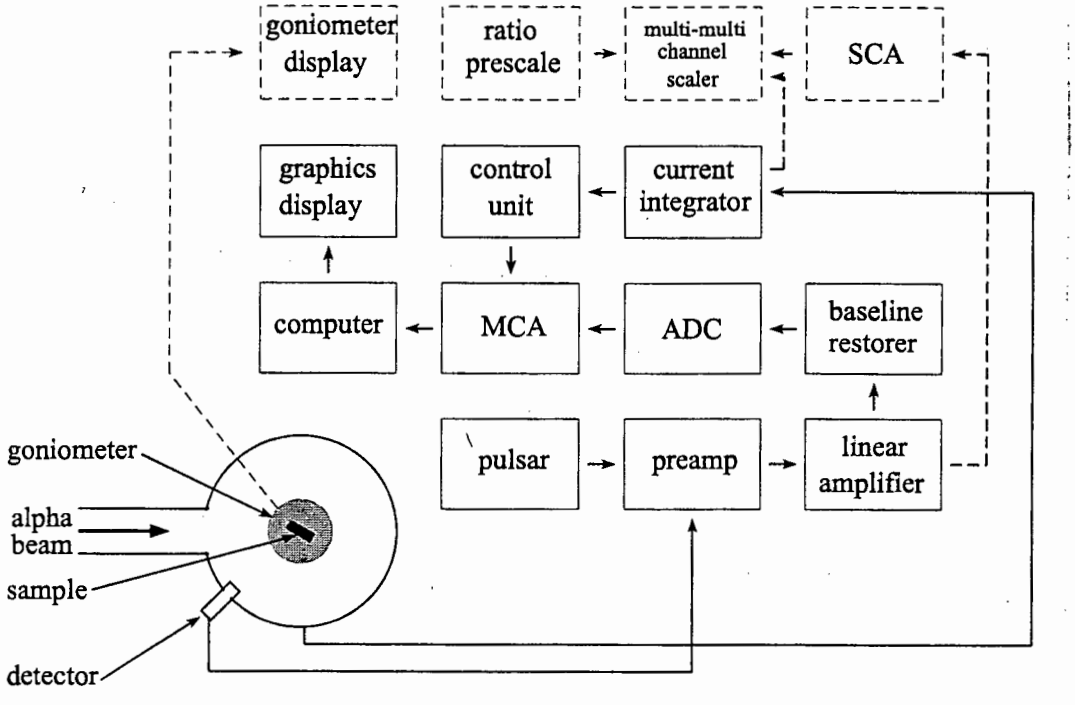

Figure 2-3: *The* **RBS** *setup.*

To perform ion beam channeling use was made of a 3 axis goniometer. A single channel analyzer (SCA) was used to gate the energy of the backscattered spectra so that the backscattered yield at any specific depth of the sample or for any particular element could be selected. The sample was aligned by x and y sweeps until a minimum was obtained. Random spectra were obtained by rotating the sample off-axis by 7°C.

2.2.2 *Dynamic* RBS

A heating stage designed to be compatible with the existing goniometer [Th95] allowed for the sample to be heated while undergoing **RBS**. The substrate heater consisted of a hollowed out cylindrical copper block about 3 cm in length containing the wound thermocoax heating elements. The whole block was surrounded by metal vanes connected to a air cooled plate which acted as a heat sink to facilitate heat dissipation.

Two K-type thermocouples were used to monitor the temperatures. One, to measure the sample temperature, was mounted on the outer surface next to the sample. The second was fixed internally, just below where the sample was mounted to measure the oven temperature. A thin conducting layer of silver adhesion paste was used to mount the sample onto the copper block. Since the **RBS** chamber serves as a Faraday cup for charge measurement, all the current carrying wires and thermocouples were isolated from the chamber. A thermal shield made from aluminium foil, with a small window, was placed over the detector to prevent any thermal radiation damage to the detector. The window in the aluminium foil was of such a size that it allowed unobstructed detection of the scattered particles but also provided maximum thermal shielding to the detector. A Eurotherm 818 temperature controller was used for the temperature control of the heating stage of the anneals.

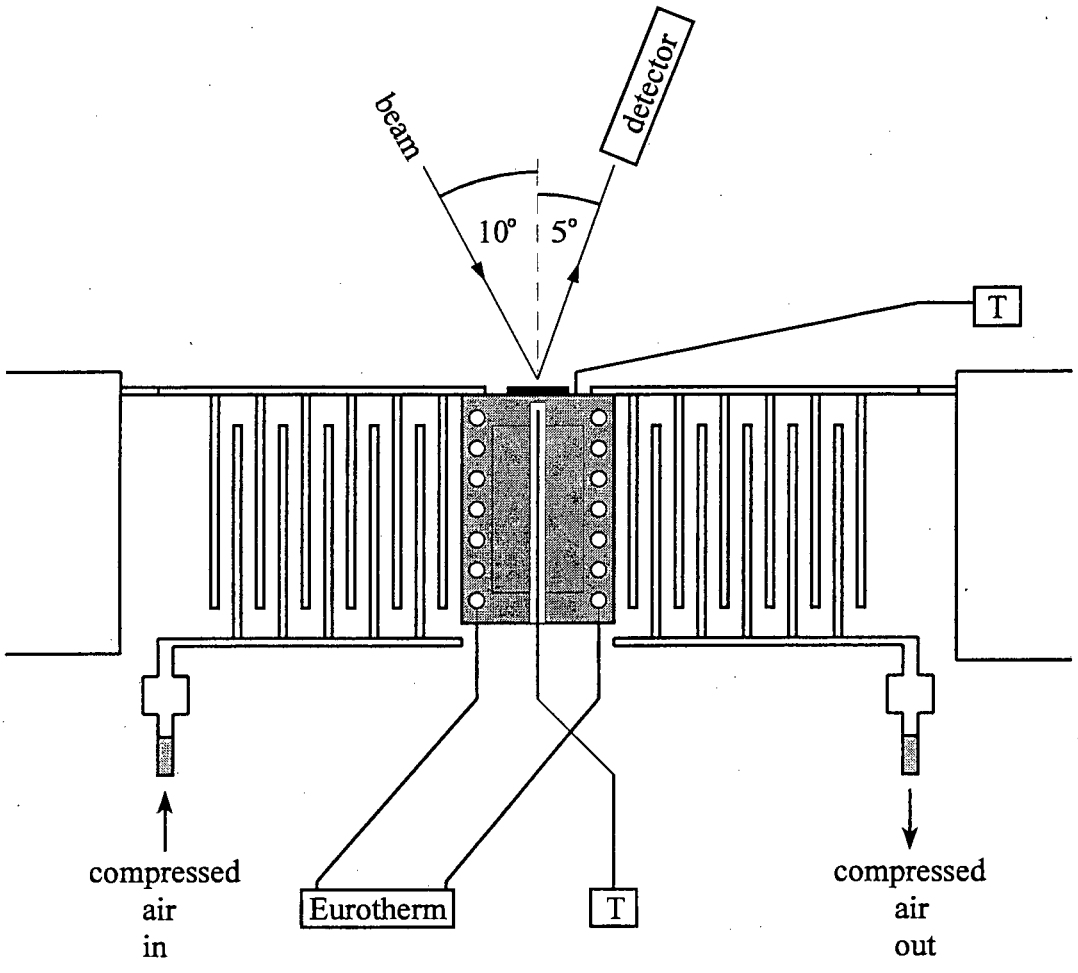

Figure 2-4: *A diagram indicating the heating stage used for Dynamic* **RBS** *measurements of solid-state interactions. The copper block containing the heating element is indicated by the large shaded area.*

Chapter 3

Preliminary Investigation

3.1 Introduction

An investigation of the thermal stability of the Cu/Pd/Si< > system has previously been performed by C-A. Chang [Ch89a]. That investigation reported that palladium and silicon diffuse into the copper, and copper accumulates under the formed Pd_2Si layer at the interface between Pd_2Si and the single crystal silicon substrate at temperatures as low as 200°C. At higher temperatures, 400°C, an extensive reaction between the copper and the above Pd_2Si was observed, forming Cu-silicides and Cu_3Pd. It must be noted that in this investigation the palladium and copper layers were deposited sequentially onto the silicon substrates, i.e. the Pd_2Si was not preformed prior to the copper deposition. In summary the report claims that the Cu/Pd/Si structures have low thermal stability and the formation of Cu-silicides and Cu_3Pd formation occurs.

These results are surprising particularly with regard to the reaction of copper with Pd_2Si to form Cu_3Pd. Since metal-metal bonds are weak in comparison to the covalently bonded Pd_2Si, it should be energetically unfavourable for the copper to break the Pd_2Si bond to form Cu_3Pd. The Pd-Si and Pd-Cu phase diagrams also suggest that this is an unlikely process.

A similar investigation was performed by Hong *et al.* [Ho94]. This investigation was concerned with a comparative study of interdiffusion and reaction in Cu/PtSi/Si< > structures. Her comparative study involved determining the copper reaction with pre-

formed PtSi on single crystal silicon substrates, i.e. comparing the reaction rates for a PtSi layer formed *in situ* and a PtSi layer formed in the furnace and then returned to the evaporator for copper deposition. The latter formation of the PtSi layer means that it has been exposed to the atmosphere before copper deposition, whereas in the first case it is not. She reported copper migration across the intermediate PtSi layer and reaction with underlying silicon to form Cu-silicides. No Cu-PtSi reaction was observed. A similar study performed by C-A. Chang [Ch89b] also reports copper migration in Cu/PtSi/Si< > structures at around 300°C.

The preliminary investigation for this study began with an investigation of the reaction between copper and preformed Pd_2Si using conventional **RBS** techniques. This was performed to obtain an indication of the type of reaction that would occur and the possible phases that might be formed. The results thus obtained by C-A. Chang [Ch89a] could be verified in terms of the copper diffusion observed, and secondly, verify any comparisons with the diffusion behaviour observed by Hong *et al.* [Ho94].

3.2 Interdiffusion and Reaction

In order to study the interdiffusion and reaction of copper with Pd_2Si, samples were prepared as described in chapter 2. The single-crystal Si<100> substrates were mounted on the substrate heater and placed in the evaporation chamber. A 500 Å layer of Pd was deposited on the silicon substrates at chamber pressures less than 10^{-7} Torr. The sample was then annealed *in situ,* without breaking vacuum, at 475°C for 30 minutes to form the Pd_2Si layer. As soon as the substrate, with the metal-silicide layer, had cooled down sufficiently (less than 70°C) a copper layer of 500 Å was deposited on top of the Pd_2Si layer. A summary of the deposition process as well as the approximate thicknesses of the deposited layers are depicted in Fig. 3.1.

It must be emphasized that the reason for *in situ* growth on the Pd_2Si and subsequent copper layer deposition was to minimize the contamination to the sample. The copper deposition is also done at a substrate temperature $T_s < 70$°C to prevent any premature reaction between the copper and the underlying Pd_2Si. Usually the samples were capped with a thin SiO_2 layer to prevent oxidation. Various samples were then

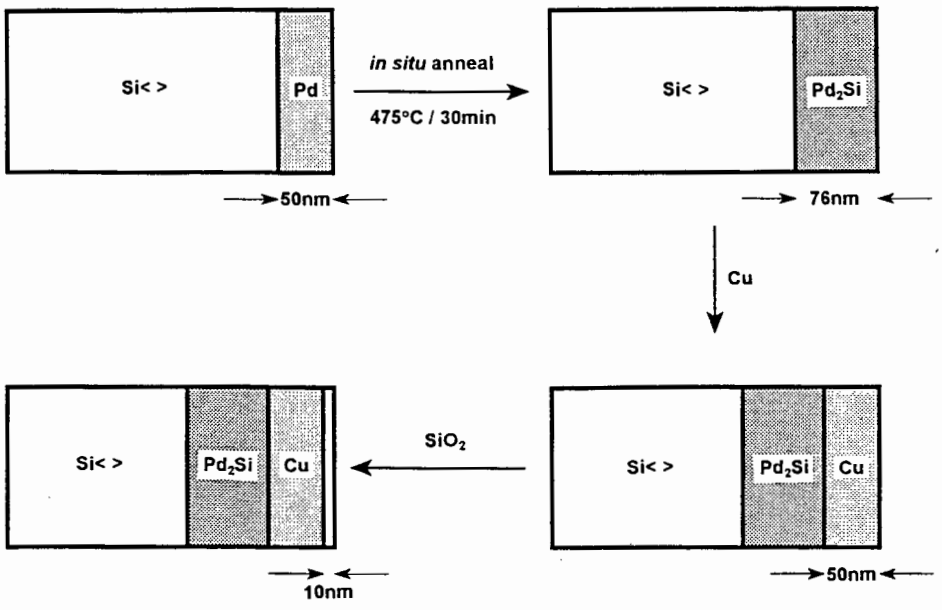

Figure 3-1: *Schematic showing the order of deposition during sample preparation. The approximate thicknesses of the various layers are also indicated.*

annealed for 20 minutes at temperatures ranging from 200°C to 300°C. **RBS** spectra following 20 minute anneals at 210°C, 220°C and 230°C are depicted in Fig. 3.2.

At 210°C the **RBS** spectra indicate evidence of the onset of reaction. There is a slight reduction in height and decrease in width of the original copper peak at channel 380 and the appearance of a smaller secondary peak at channel 350. Simultaneously it is observed that the Pd_2Si signal also moves to higher energies. The decrease in the copper signal at channel 380 indicates the loss of copper from the surface layer and the appearance of the copper peak at channel 350 indicates a Cu-Si reaction at the $Pd_2Si/Si< >$ interface, indicating that there is copper transport across the barrier layer. The apparently improved resolution of the copper and palladium signals as the reaction proceeds is due to the Pd_2Si layer moving to the surface while the 'surface' copper peak is narrowing due to its diffusion from the surface across the barrier layer. This results in a decrease in the overlap of the palladium and copper signals in the **RBS** spectra.

Since the spectra indicate no build up of copper in the Pd_2Si layer, this would suggest that there is no reaction between the copper and the Pd_2Si layer. The entire

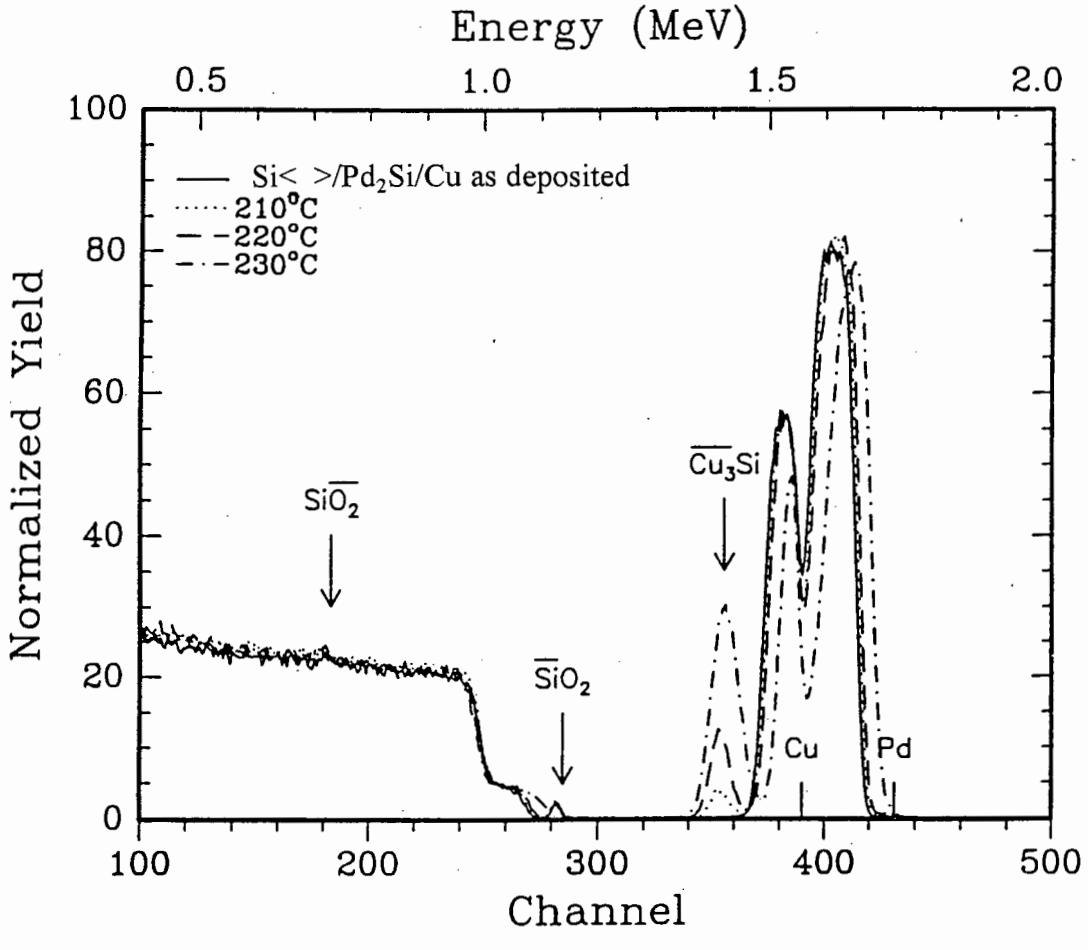

Figure 3-2: *Selected* **RBS** *spectra indicating the diffusion of Cu through* Pd_2Si *and subsequent growth of the Cu-silicide. The samples were annealed in the temperature range 200° C - 300° for 20 minute intervals.*

palladium peak appears to move uniformly to the surface which suggests that the copper diffuses uniformly through the barrier layer. The Pd_2Si layer appears to retain its original composition and original thickness. The rapid diffusion of copper into the silicon substrate also appears to be very temperature dependent, as seen by the large change in the amount of copper that has diffused through following small increases in annealing temperature. The onset temperature for reaction is low which would indicate that the system is highly reactive. This is consistent with findings in a similar investigation [Ho94].

These preliminary results indicate that the copper does not react with the Pd_2Si layer, but diffuses through the Pd-silicide layer to the $Pd_2Si/Si< >$ interface at relatively low temperatures (around 200°C) as indicated in Fig. 3.3. The rate of copper diffusion through the silicide layer was found to increase rapidly with annealing temperature. Previous work has reported the first Cu-silicide phase to form at these low temperatures is Cu_3Si [Ya94, Ch90, Ho91, St91]. X-ray diffraction was performed on these samples, but identification of the silicide was not possible due to the limited thickness of the films. It was therefore assumed that Cu_3Si was formed at the $Pd_2Si/Si< >$ interface. The driving force for this diffusion reaction can be attributed to the high affinity copper has for silicon.

3.3 Influence of Pd_2Si structure on Cu Diffusion

The next stage of the preliminary investigation was performed to determine whether the structure of the interposed Pd_2Si layer had any influence on the rate of diffusion of copper through the silicide layer. To do this, the Pd_2Si layer was grown on Si<111> and Si<100> substrates. A detailed discussion concerning the epitaxy of Pd_2Si on Si<111> has been presented in section 1.1.2. In order make the comparison valid, care was taken to prepare the samples under identical conditions. This was achieved by simultaneously mounting both silicon substrates on the substrate heater, thereby ensuring identical deposition conditions. Therefore, the thicknesses of the Pd_2Si and copper films on the Si<111> and Si<100> substrates was identical as well as the substrate heat treatment. The Pd_2Si layer was grown on both substrates *in situ* at

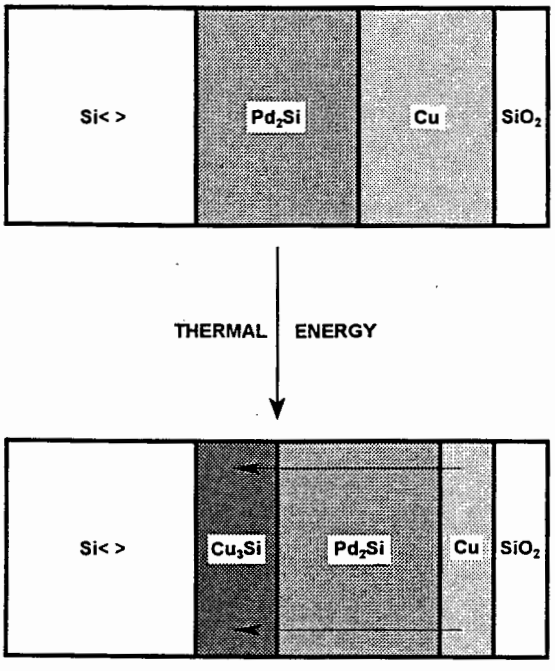

Figure 3-3: *A graphical representation of the Cu diffusion through the intermediate Pd_2Si layer and subsequent formation of the Cu-silicide layer at the $Pd_2Si/Si<>$ interface.*

450°C in the evaporator followed by depositing the copper layer.

After removal from the evaporator the samples were then subjected to a further anneal for 20 minutes each at temperatures ranging from 175°C to 400°C. Selected **RBS** spectra from this investigation are shown in Fig. 3.4 and Fig. 3.5. It should be noted that these eight samples were not capped with a SiO_2 layer.

As can be seen in Fig. 3.4, that for samples prepared on the Si<100> substrate, the copper diffusion across the silicide barrier layer again began at a fairly low temperature of about 200°C. The sample prepared on the Si<111> substrate at the same temperature shows no evidence of copper diffusion. The onset of the copper diffusion process on the Si<111> substrate was first observed at 225°C, whereas the reaction is quite considerable at the same temperature on the Si<100> substrate. In both cases the general behaviour observed was similar to that reported earlier in section 3.2.

The experiment was repeated a number of times with similar results viz. onset of copper diffusion and reaction occurred at temperatures of 20°C to 30°C lower on

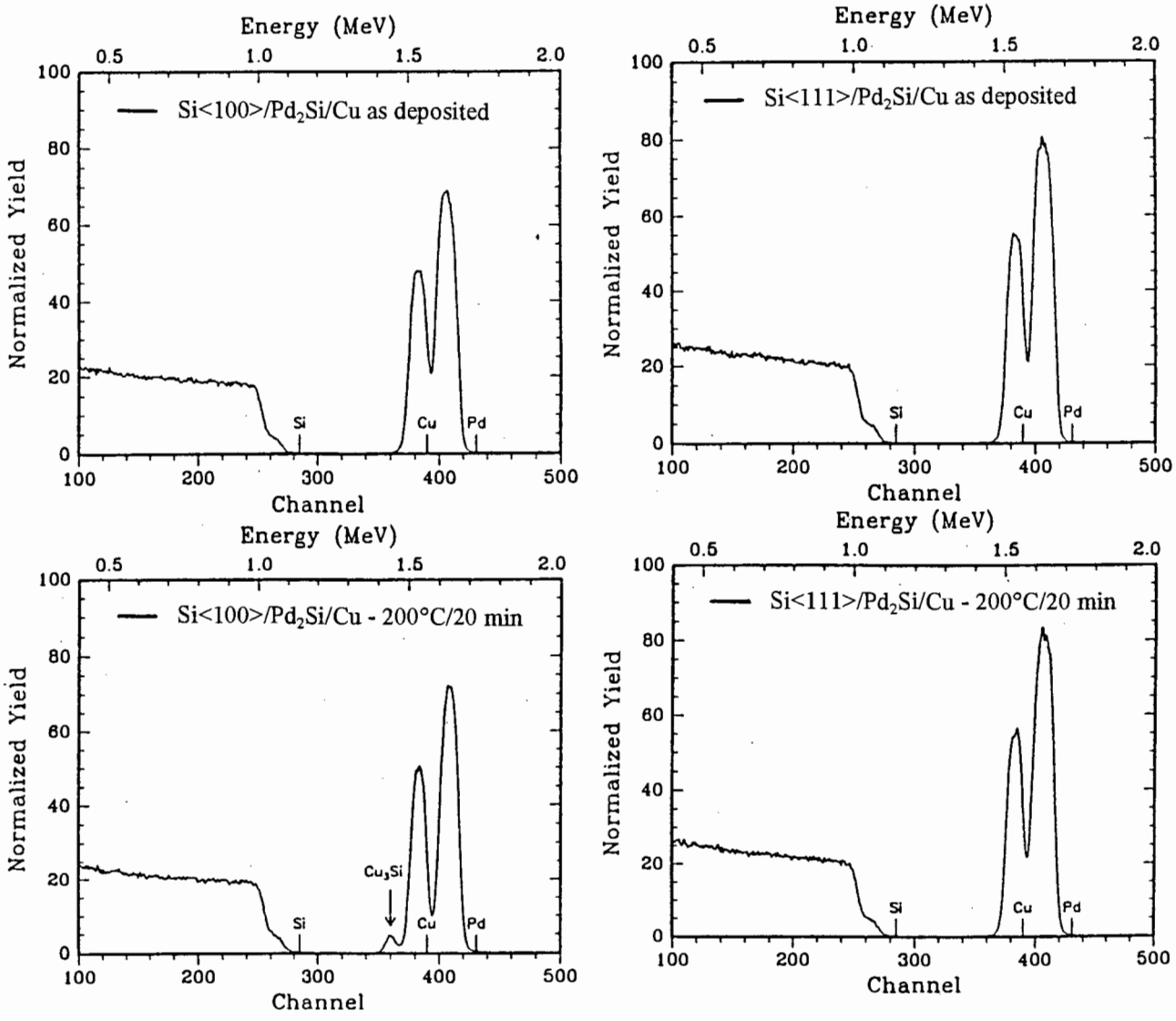

Figure 3-4: *Comparative* **RBS** *spectra for samples grown on Si<100> and Si<111> substrates. The temperature range for vacuum furnace annealing was 190° C - 250° C for 20 minutes. The spectra shown here are as deposited and 200° C. The spectra indicate the onset temperature for Cu diffusion is lower for Si<100> compared with Si<111>.*

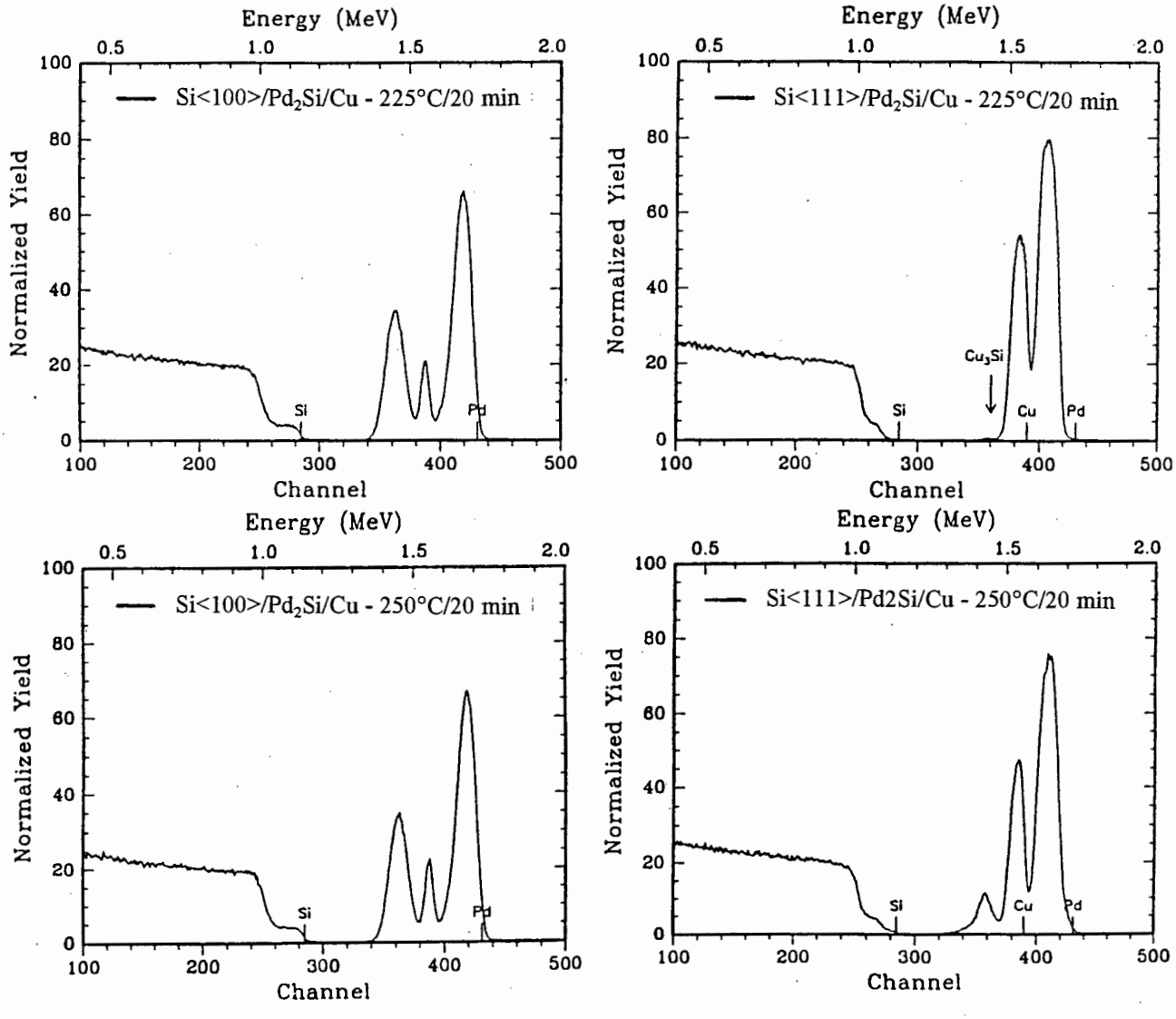

Figure 3-5: *Comparative* **RBS** *spectra for samples grown on Si<100> and Si<111> substrates. The spectra shown here had been annealed for 225° C and 250° C. The spectra indicate increased Cu diffusion on Si<100> compared with Si<111>.*

Si<100> than on Si<111>. Further **RBS** spectra of a different experimental run are displayed in Fig. 3.6 where the temperature difference is again clearly visible. In this case the samples were coated with an SiO_2 layer to prevent oxidation. One can see that the amount of copper that has diffused through the Pd_2Si layer (on Si<100>) at 210°C is comparable to the amount that has diffused through on the Si<111> substrate at 230°C. This would indicate the same or comparable amount of copper diffusion. Given that all the samples were annealed for 20 minutes, it is clear that under these annealing conditions the temperature at which the presence of the copper silicide is first observed by **RBS** differs by approximately 20°C. This observed temperature difference is shown in Fig. 3.6. It should be noted that although the temperature difference was similar from one experimental run to another, the precise temperature at which the copper silicide was first observed differed slightly from run to run.

From this investigation the results strongly suggest that there is a difference in reaction rates for copper diffusion through Pd_2Si grown on the two different substrate orientations.

3.4 Copper Reaction with Silicon Substrate

Earlier work by C-A. Chang suggests that there is an orientation dependence for the Cu-Si reaction, i.e. the silicide formation rate is about five times faster for <100> orientated substrates than for the <111> substrates at 200°C [Ch90]. An interpretation of the observed results is that it is possible that the observed difference in the reaction rates on the two substrate orientations is a result of the Cu-Si interaction, and not a consequence of the crystal quality of the interposed Pd_2Si layer which could affect the diffusion through the layer. So the difference in temperature at which Cu_3Si formation is first observed could be due to the different rates of reaction of copper with the silicon substrate.

To check the validity of this claim the reaction of copper on the two silicon substrate orientations was investigated. Copper films, 500 Å thick were deposited on Si<100> and Si<111> substrates at room temperature. The substrates were both mounted simultaneously for the deposition to allow a direct comparison of the deposited films.

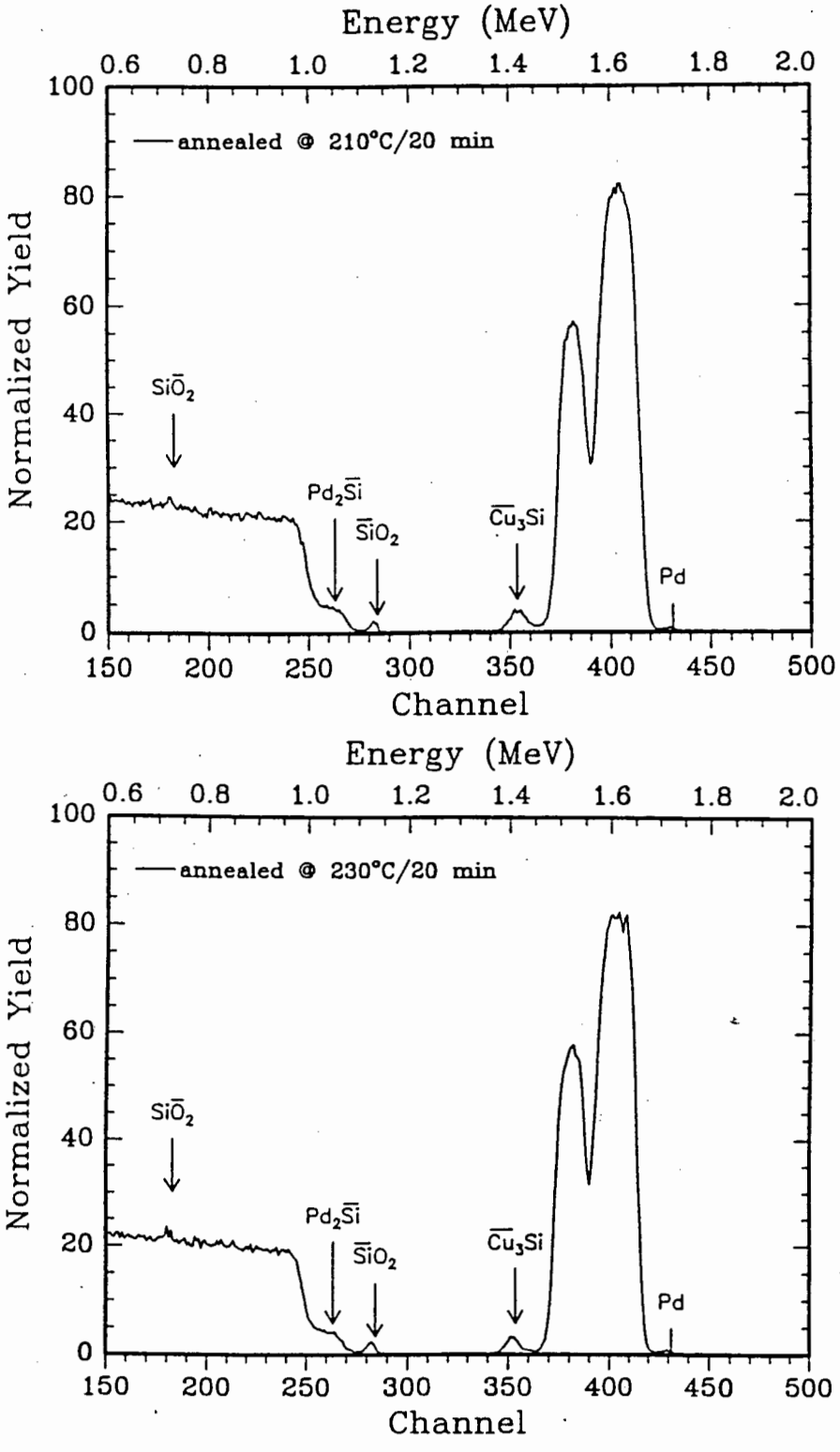

Figure 3-6: **RBS** *spectra indicating a direct growth comparison for the two different substrate orientations. For two different temperatures roughly the same amount of growth is observed indicating an approximate 20° C difference in the observed starting temperature for copper diffusion.*

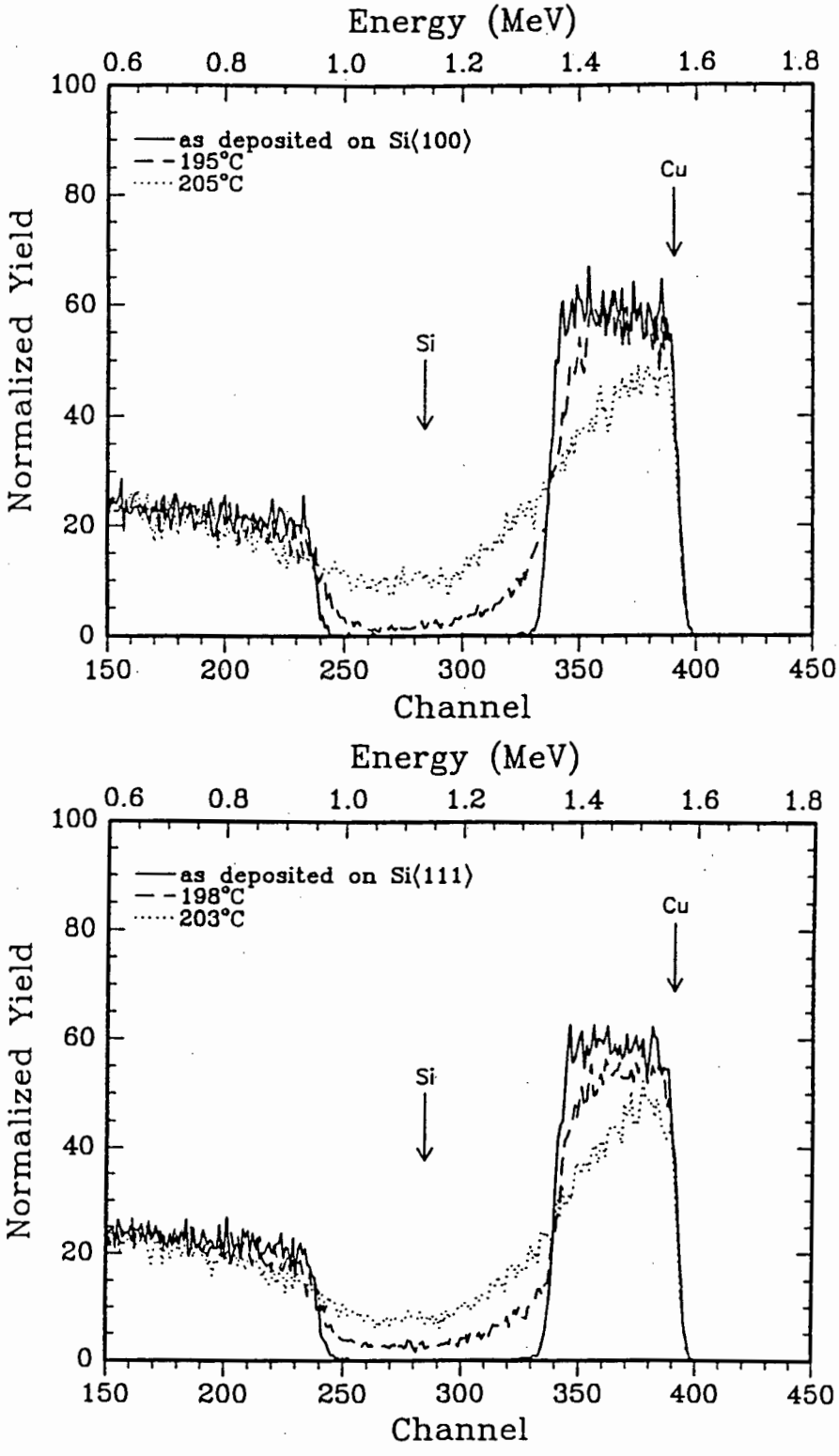

Figure 3-7: *Comparative* **RBS** *spectra for copper reaction with Si<100> and Si<111> substrates. Visually their appears to be no difference between the copper reaction with the two silicon substrates.*

The samples were then annealed between 180°C and 210°C in vacuum. The narrow temperature range was chosen because copper is highly reactive with silicon. Selected **RBS** spectra of the comparison are shown in Fig. 3.7.

In both cases it appears that the copper diffuses rapidly into the silicon substrate over a very short time period and the spectra indicate that the reaction is non-uniform. This non-uniformity could possibly be due to 'balling' of the thin film layer. It is never the less observed that the onset temperature of the reaction is the same for both substrates and that the 'growth rates' of the Cu-silicide are also the same.

From the above observations we can deduce that there is no valid support for the claim that the copper reacts differently on Si<100> and Si<111>, since the above results indicate that there is no significant difference in the onset temperature and reaction rate between copper and silicon on the two orientations. The observed difference in the diffusion rates and growth of the copper-silicide grown on the two different substrate orientations is therefore most likely due to the microstructure of the Pd_2Si layer.

3.5 Channeling in Pd_2Si layer

The objective for channeling measurements in the Pd_2Si layer was to check whether the epitaxial quality of the Pd_2Si thin film varied as the reaction proceeded and to establish whether there was any Cu-Pd_2Si interaction.

The two samples that underwent channeling were prepared as shown in Fig. 3.1. It must be noted that these samples were prepared on the Si<111> substrate. One sample was as deposited and the other was annealed in the vacuum furnace at 250°C for 120 minutes to obtain the diffusion reaction. The surface copper layer was then etched off both samples using a dilute nitric acid solution to expose the underlying Pd_2Si layer. The channeling spectra obtained from these two samples are shown in Fig. 3.8a and b.

A minimum yield (χ_{min}), the ratio of aligned yield to random yield (Y_a/Y_r), of approximately 55% was obtained from the as grown Pd-silicide sample shown in Fig. 3.8a. This indicated a reasonable epitaxial quality of the palladium silicide layer grown on

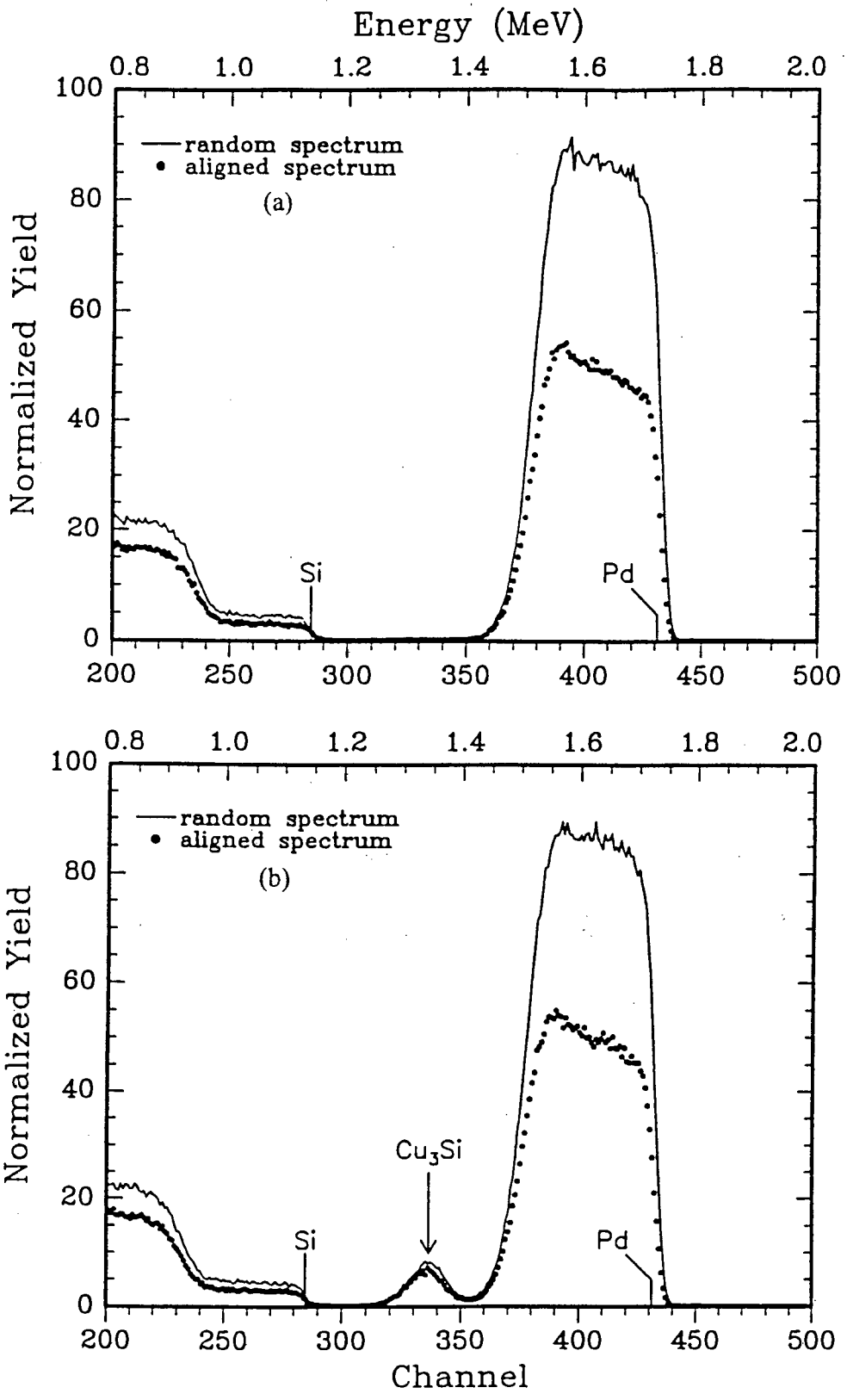

Figure 3-8: *Comparative* **RBS** *channeling spectra, random and aligned for (a) as grown Pd-silicide and (b) after the diffusion reaction. The minimum yield,* $x_{min} \sim 55\%$ *indicates reasonable epitaxial quality of the* Pd_2Si *layer.*

the Si<111> substrate given that the Pd_2Si layer was prepared at a relatively low temperature of 450°C. In Fig 3.8b the value of the minimum yield after the diffusion reaction is likewise approximately 55%.

This channeling data provides conclusive evidence that firstly, the Pd_2Si layer does grow epitaxially on Si<111>, and that the quality of the epitaxy is reasonably good. Secondly, that the epitaxial Pd_2Si structure is not influenced by the copper diffusing across it to grow at the Pd_2Si/Si< > interface. It is as if the epitaxial Pd_2Si layer just 'floats' off the Si< > substrate. There is also evidence to support a lack of copper incorporation in the Pd_2Si layer. This is indicated by no change in χ_{min}, i.e. the minimum yield before and after diffusion reaction is the same.

3.6 Reaction Kinetics

The observation that the choice of silicon substrate on which the Pd_2Si layer was grown could influence the rate of copper diffusion proved very interesting. Determining the diffusion mechanism on the two different substrate orientations would provide a better understanding of the influence of the substrate. One way would be to determine the activation energies for copper diffusion through Pd_2Si and subsequent Cu-silicide formation on the two different substrate orientations. If the activation energies are equivalent (within experimental uncertainty) then the diffusion mechanism are also likely to be the same for the two Pd_2Si structures on Si<100> and Si<111>. Alternatively if the diffusion mechanism is different for either structure then one would expect the activation energies to differ as well. If, however the diffusion mechanism is the same, then a possible reason for the difference in onset temperature could be the microstructure of the Pd_2Si film. The activation energies are easily determined by plotting the growth rates of the Cu-silicide layer in an Arrhenius plot.

The samples were prepared as before, i.e. simultaneous *in situ* anneal to form Pd_2Si followed by copper and SiO_2 deposition. They were then further annealed (using a conventional furnace) at three different temperatures, 190°C, 200°C and 210°C, for times ranging from 10 to 90 minutes. It must be pointed out that the investigation was only carried out on the Si<100> substrate.

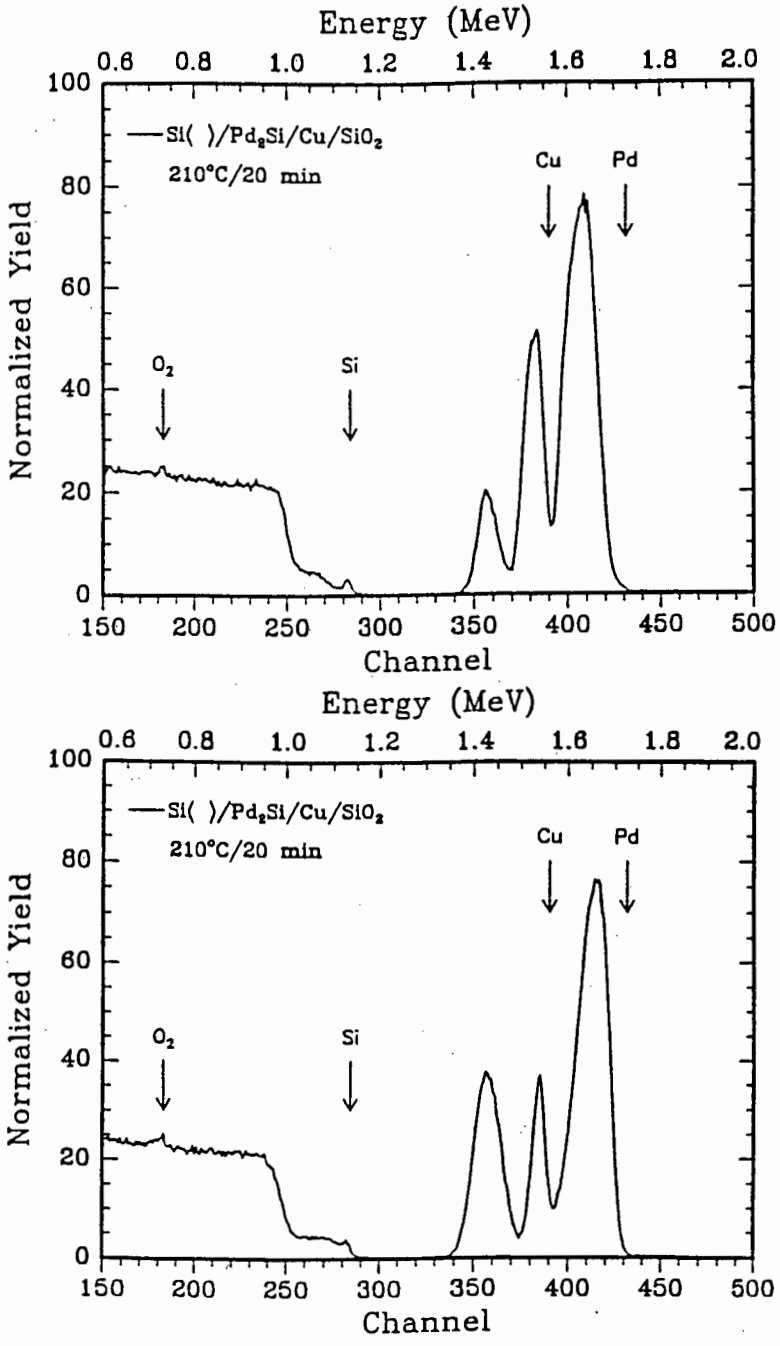

Figure 3-9: **RBS** *spectra for two different samples prepared under the same conditions, i.e. identical temperature and annealing time. Note that the growth on the one sample appears to be greater although they experienced the same annealing conditions.*

The first major obstacle encountered in this investigation was the irreproducibility of results. **RBS** spectra from two samples annealed at 210°C for 20 minutes in the vacuum furnace in the same boat can be seen in Fig. 3.9. One would assume under similar conditions they would exhibit the same amount of Cu-silicide growth, however as shown in Fig. 3.9 this is clearly not observed.

One possible explanation for this behaviour could be that with this highly reactive system (highly temperature sensitive), a slight non-uniform temperature distribution along the length of the boat could lead to these spurious results. To check whether this would explain the observed results, three samples were loaded in each boat as indicated in Fig. 3.10. The sample in the middle of the quartz boat was directly below the thermocouple which is positioned at the centre of the furnace. Either side of the furnace was also sealed with glass wool in an attempt to maintain as uniform temperature as possible inside the furnace.

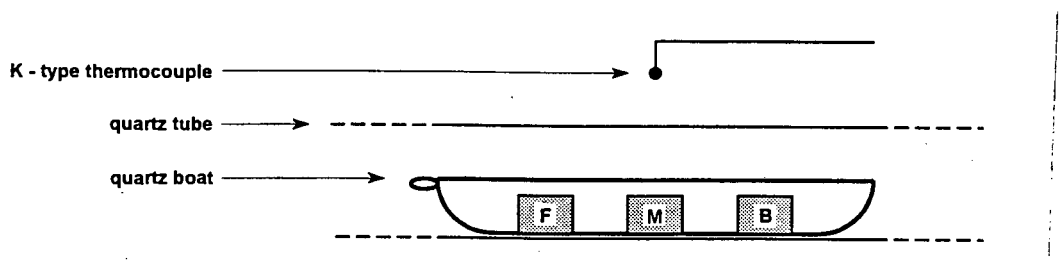

Figure 3-10: *A quartz boat sample holder containing three samples. Note that the middle sample is directly below the thermocouple.*

A plot of the data acquired for a 220°C anneal is shown in Fig. 3.11. The plot shows the fraction of copper that has diffused through the Pd_2Si layer as a function of annealing time for the three samples front, middle and back of the quartz boat. One observes that at 20 minutes the fraction of copper reacted for the sample in the front position is greater than that for the sample at the back. The reverse is true for samples annealed for 30 minutes. Clearly if there was a temperature gradient across the length of the boat then one would expect all the samples in the front position to occupy roughly the same position on the plot with respect to the samples on the

back position. Since there is no consistent pattern in the data, the observed variation cannot be attributed to a temperature gradient across the length of the quartz boats. This variation could be due to various factors; the quality of the Pd_2Si layer, varying annealing conditions or even the presence of impurities or native oxides which will all cause the samples to differ considerably from one another. The extent of the scatter in the data is so great that it does not allow the activation energy to be determined.

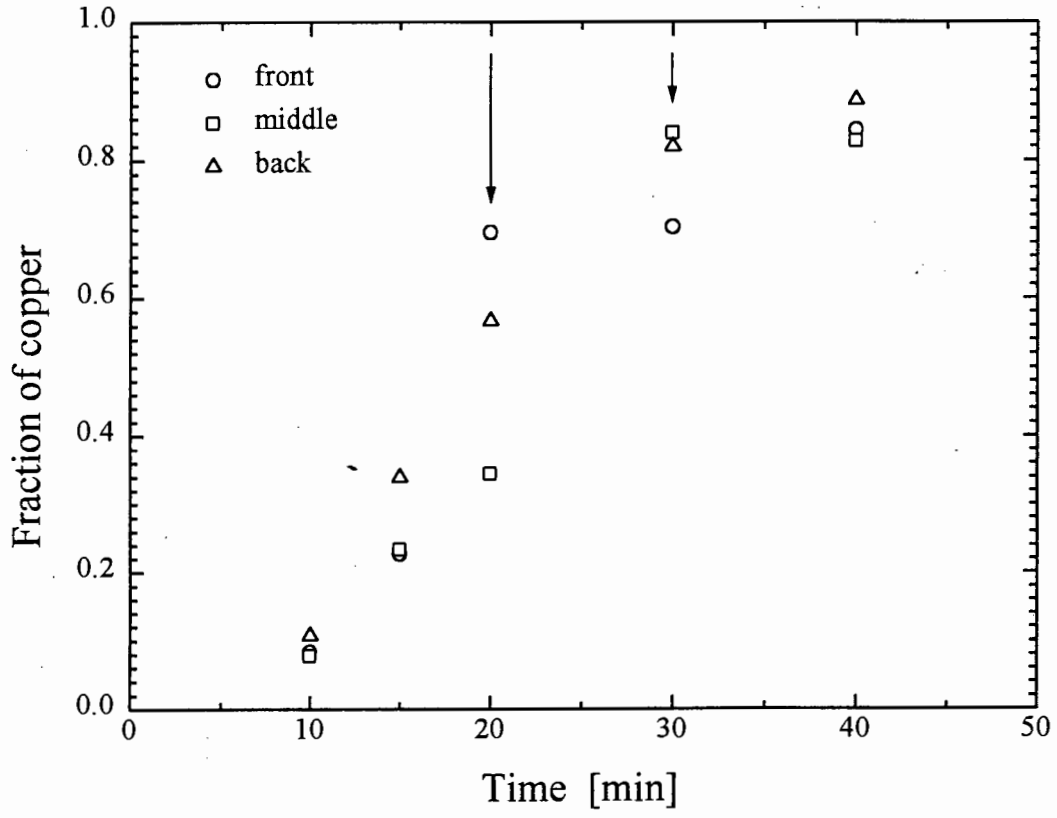

Figure 3-11: *A plot of the fraction of copper that has diffused through the intermediate Pd_2Si layer as a function of annealing time. There appears to be no direct relationship between the fraction of copper and time.*

3.7 Summary

The preliminary investigation showed that copper diffused through the Pd_2Si layer without interaction. Evidence of the Cu-Si reaction is apparent from the data but identification of the phase formed at the $Pd_2Si/Si<>$ interface was not determinable from **RBS**. A difference in the onset temperatures for copper diffusion across this layer for samples grown on differently orientated substrates, i.e. Si<100> and Si<100>, was also observed. From the results presented in section 3.4 the selective $Cu/Si<>$ interaction as a possible reason for this difference can be ruled out, indicating that the difference in onset temperature is possibly due to the structure of the interposed Pd_2Si layer.

The microstructure of Pd_2Si could be the possible cause of this difference in onset temperatures since Pd_2Si only grows epitaxially on Si<111> substrates whereas it does not on Si<100> substrates. As discussed in section 1.1.2 the Pd_2Si grown epitaxially on Si<111> has lower angle grain boundaries compared with Pd_2Si grown on Si<100>. By looking at Fig. 1.2 it is evident that the cross-sectional area of the region between the grains has an angular dependence. If this angle is small (i.e. low angle grain boundaries) the cross-sectional area between the grains is small. The opposite would be true for larger angle grain boundaries. Therefore if copper diffuses via grain boundary diffusion then it would be logical to expect that these low angle grain boundaries in epitaxially grown Pd_2Si could inhibit the copper diffusion. Hence there are two possibilities that arise; 1) that the two growth mechanisms are entirely different, or 2) that the growth mechanisms are identical with the diffusion inhibited in the case of Si<111> for the reasons discussed above. The latter possibility would indicate grain boundary diffusion for Si<100> and bulk diffusion for Si<111>. It must be noted that their is an appreciable difference between the activation energy for grain boundary and bulk diffusion. So determining the activation energy for copper silicide formation in both cases should provide a means of distinguishing between the two mechanisms. Due to the irreproducibility of the results however it was not possible to determine the activation energy for copper diffusion.

The copper diffusion process was sensitive to any variations since the data acquired

was noisy and irreproducible. The large variation from sample to sample meant that it was not possible to claim with complete certainty that the copper diffusion across Pd_2Si grown on the two substrate orientations was different. Possible variations between samples could be :

(i) initial experimental conditions,

(ii) temperature and duration of annealing,

(iii) impurities e.g. oxide layers present at interfaces and

(iv) the epitaxial quality of the Pd_2Si layer varying across the lateral dimensions of the sample.

Since the copper-silicon reaction takes place at low temperatures, it seems reasonable to expect that it is sensitive to small variations from sample to sample. Due to the lack of reproducibility of experimental results other means of sample analysis needed to be pursued.

Chapter 4

Dynamic RBS study of copper diffusion

4.1 Introduction

As discussed in the previous chapter the variations from sample to sample led to statistically unreliable results. To eradicate the need for multiple samples and the problem of non-uniform reactions using this conventional method another experimental technique was pursued. The technique, involving **RBS**, will be referred to in this text as *dynamic* **RBS**. The term *dynamic* **RBS** involves continuous **RBS** while the sample is undergoing a thermal anneal [Th95]. The technique can be applied to samples kept at a constant temperature during **RBS** analysis or to samples subjected to a constant 'temperature ramp' during **RBS** analysis. The latter will be referred to as 'temperature ramping'.

The advantages of using this technique was that (i) fewer experimental runs were needed for analyzing reaction kinetics, (ii) the temperature range in which the reaction occurred was easily identifiable and, (iii) the reaction can be observed in real time. This is particularly useful for preliminary investigation to establish the most desireable conditions for analysis. The second advantage is of particular importance since with conventional means this reaction region or onset temperature is not clearly identifiable and hence accurate kinetics cannot be easily established. This technique will be de-

scribed briefly in terms of the study pursued in the work. The experimental setup of the real time *dynamic* **RBS** was discussed in chapter 2. By applying this technique the activation energy and the growth mechanism could be determined. It was also used to confirm whether their is a difference in onset temperature for copper diffusion through Pd_2Si grown on Si<100> and Si<111> substrates.

4.2 *Dynamic* RBS

The technique allows the analysis of a single sample by continuous **RBS** during the anneal i.e. *in situ* **RBS.** The as prepared sample was mounted on the substrate heater as shown in Fig. 2.4 and placed into the vacuum chamber. When the chamber pressure had dropped to approximately 10^{-5} Torr the sample characterization procedure could begin. The sample temperature was raised rapidly to 200°C at a rate of 20°C/min and thereafter at a constant rate of 1°C/min (dT/dt) to 310°C. It must be noted that the ramp rates and temperature ranges were those that pertain directly to this investigation and could be easily adapted for other studies. While the sample was undergoing heating it was continuously monitored by **RBS**. After all the data was captured the heater was switched off and the sample allowed to cool before being removed.

When applying this technique it is assumed that the mode of reaction remains unchanged and that the phase formed is the same throughout the temperature range scanned. This is very important because if the ramping rate is high, the shorter annealing time at lower temperatures must be compensated by ramping to higher temperature. At these higher temperatures the risk is greater that their might be a change in the mode of reaction or phase produced. To avoid this risk the ramping rate was kept sufficiently low, in this case 1°C/min.

As described in section 2.2.2 the temperature was measured at two positions during the experimental runs, referred to here as the 'sample' and 'oven' temperature. The thermocouple measuring the oven temperature was mounted internally in the copper substrate block on which the sample is mounted, while the sample temperature was measured by a thermocouple mounted on the outer surface next to the sample. A plot of the heating temperature, sample and oven temperature, as a function of time for

a typical experimental run is shown in Fig. 4.1. From the figure it is observed that their is a difference of 10 – 20°C between the sample and oven temperatures. This difference appears to increase with temperature. The temperature difference could be attributed to the temperature gradient through the copper substrate block from the inner to outer surface. It is also possible that some heat is lost due to conduction and radiation at the surface, or that there is a poor contact between the copper substrate and the sample thermocouple. However the temperature difference is observed to vary consistently from one experimental run to another.

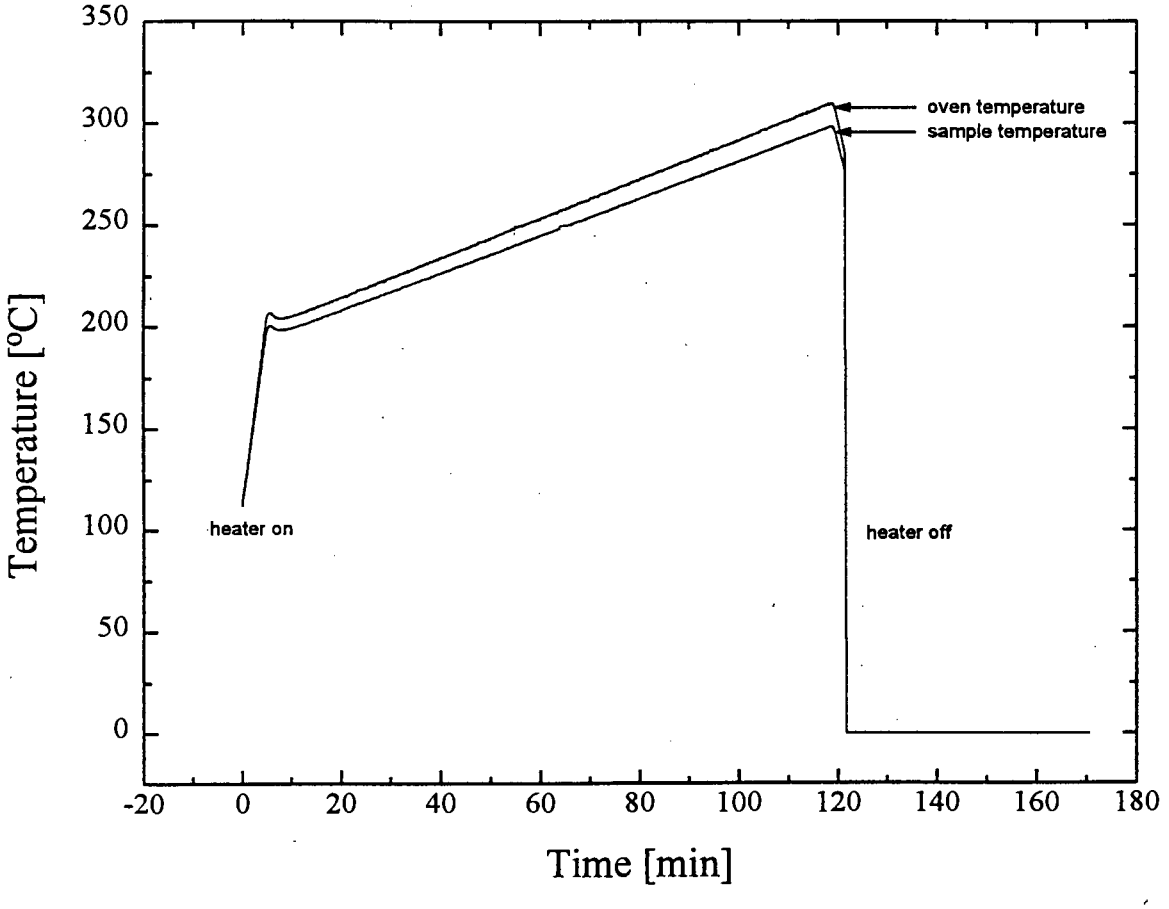

Figure 4-1: *A graph of the oven and sample temperature as a function of time. The oven temperature was ramped from 200° C to 310° C at 1° C/min.*

RBS spectra were accrued in 10 second intervals and stored in a two dimensional array. After the experimental run was complete it was then possible to group the spectra into larger time intervals, 1 or 2 minutes, to provide better statistics. These spectra were then charge-normalized to compensate for current variations and con-

verted to a format that made the method of analysis suitable for the **RUMP RBS** fitting program. A typical **RBS** spectrum that is obtained using this technique is shown in Fig. 4.2. In this particular case the spectra were grouped into 2 minute intervals, hence the spectrum shown is actually twelve 10-second spectra. It is clear that there is still some scatter in the data. However the large number of data points more than offsets the uncertainty due to the scatter in the data, allowing easier fitting of a best-fit straight line to the generated Kissinger plots. A typical number of data points would be between 20 and 30.

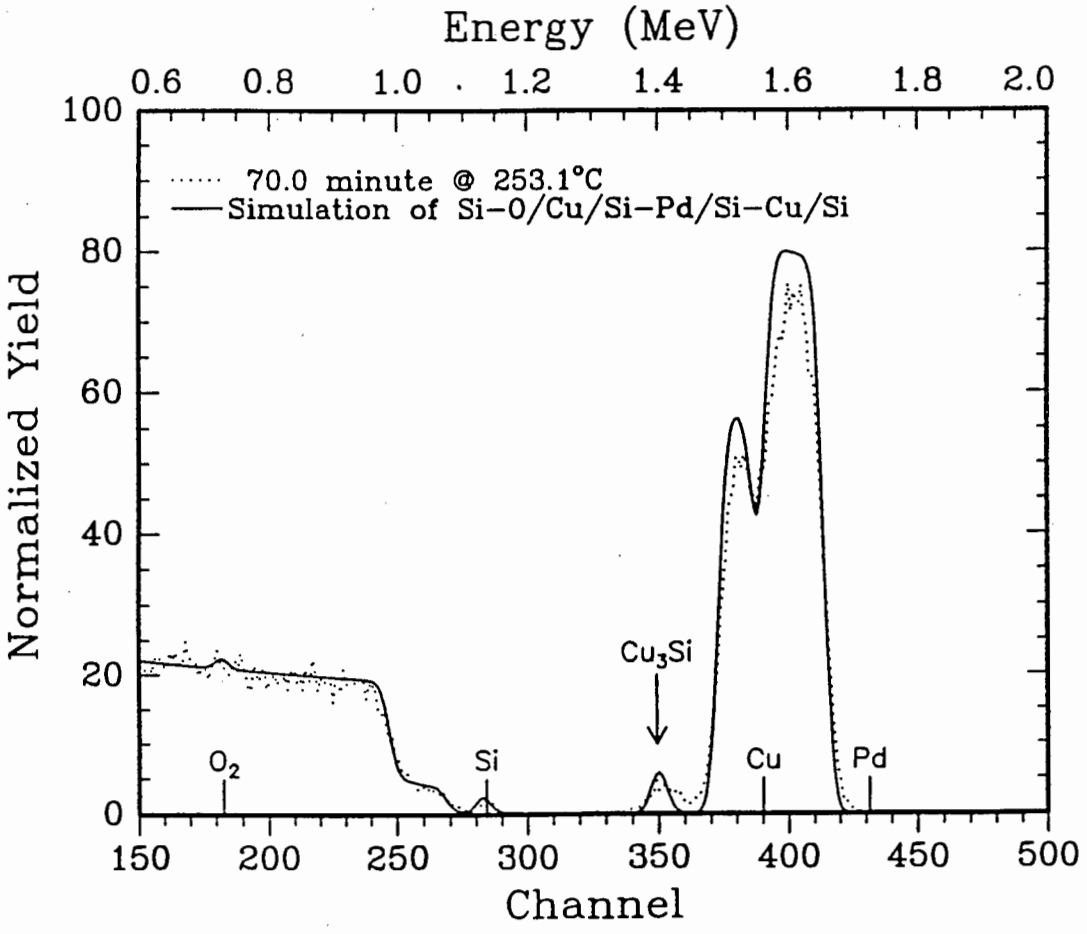

Figure 4-2: *A typical* **RBS** *spectrum obtained after grouping and charge-normalization with the accompanying simulation. The temperature indicated is the average sample temperature reading after 70 minutes.*

The data provides a novel three dimensional plot, which are the individual, 1 or 2 minute spectra plotted as a function of time. These plots are depicted in Fig. 4.3 and Fig. 4.4 for copper diffusion through Pd_2Si grown on Si<100> and Si<111> substrates respectively.

In Fig. 4.3, all the features previously described in section 3.2 can be seen. At approximately 70 minutes the copper diffusion begins, as apparent by the appearance of a copper peak at an energy value of approximately 1.43 MeV. This secondary copper peak becomes progressively larger. Although it appears from this plot that the primary copper peak counts drop off suddenly, this is an artifact of the plot, because as can be seen the secondary peak increases gradually, indicating a well behaved reaction. The silicon peak in the SiO_2 and the silicon peak in the Pd_2Si are also well separated before the reaction begins. But as the reaction time proceeds, the silicon peak in the Pd_2Si appears to move to higher energies causing a smearing of the silicon peak into the substrate. This motion of the Pd_2Si shifting to a higher energy is also clearly evident.

Similar features are also evident in Fig. 4.4. The major visible difference between the two is the observed starting temperature, (proportional to time from ramp rate), for copper diffusion. On the Si<100> substrate this occurs at approximately 65 min and approximately 80 min for Si<111>. In addition the growth rate of the secondary copper peak for Si<100> increases monotonically. This is to be expected since the temperature is increasing at a constant rate. The growth rate for the secondary copper peak for Si<111> is however somewhat different. It increases steadily during the initial stages of diffusion up to about 100 minutes where the growth rate increases suddenly to a higher value indicating a more rapid growth of the secondary copper peak. The source of this change is not clearly understood. This could indicate a changeover in the growth mechanism of the copper silicide.

4.2.1 Influence of beam heating

It is clear that the samples spend long periods of time, up to 120 minutes, undergoing **RBS** during analysis. The question could then be asked whether the beam has any long term influence on the reaction that is being investigated. What is meant by

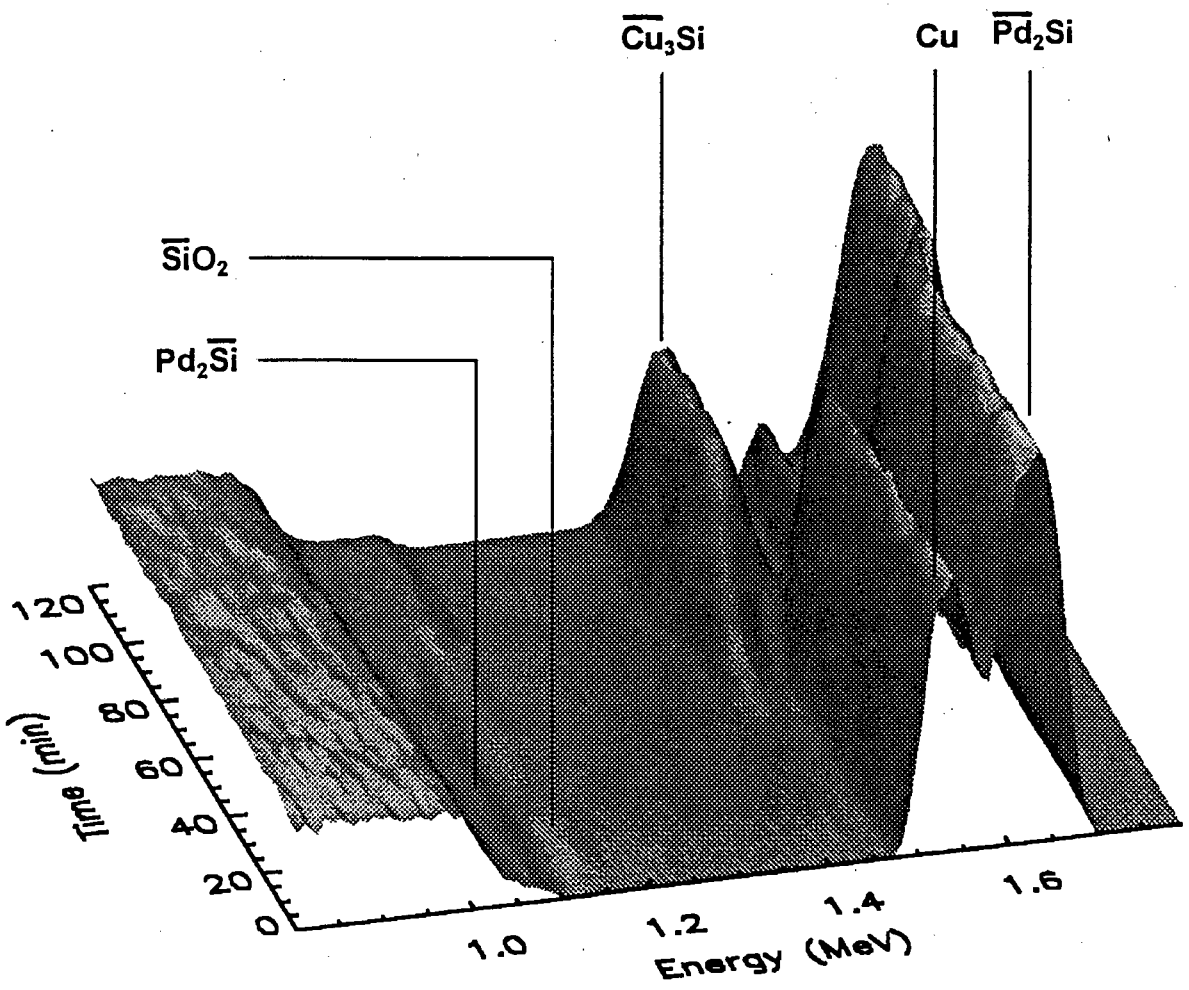

Figure 4-3: *A plot indicating the continuous* **RBS** *spectra as a function of time for the Si<100> substrate. The* **RBS** *spectra were grouped in two minute intervals. The copper diffusion through Pd_2Si is clearly observed.*

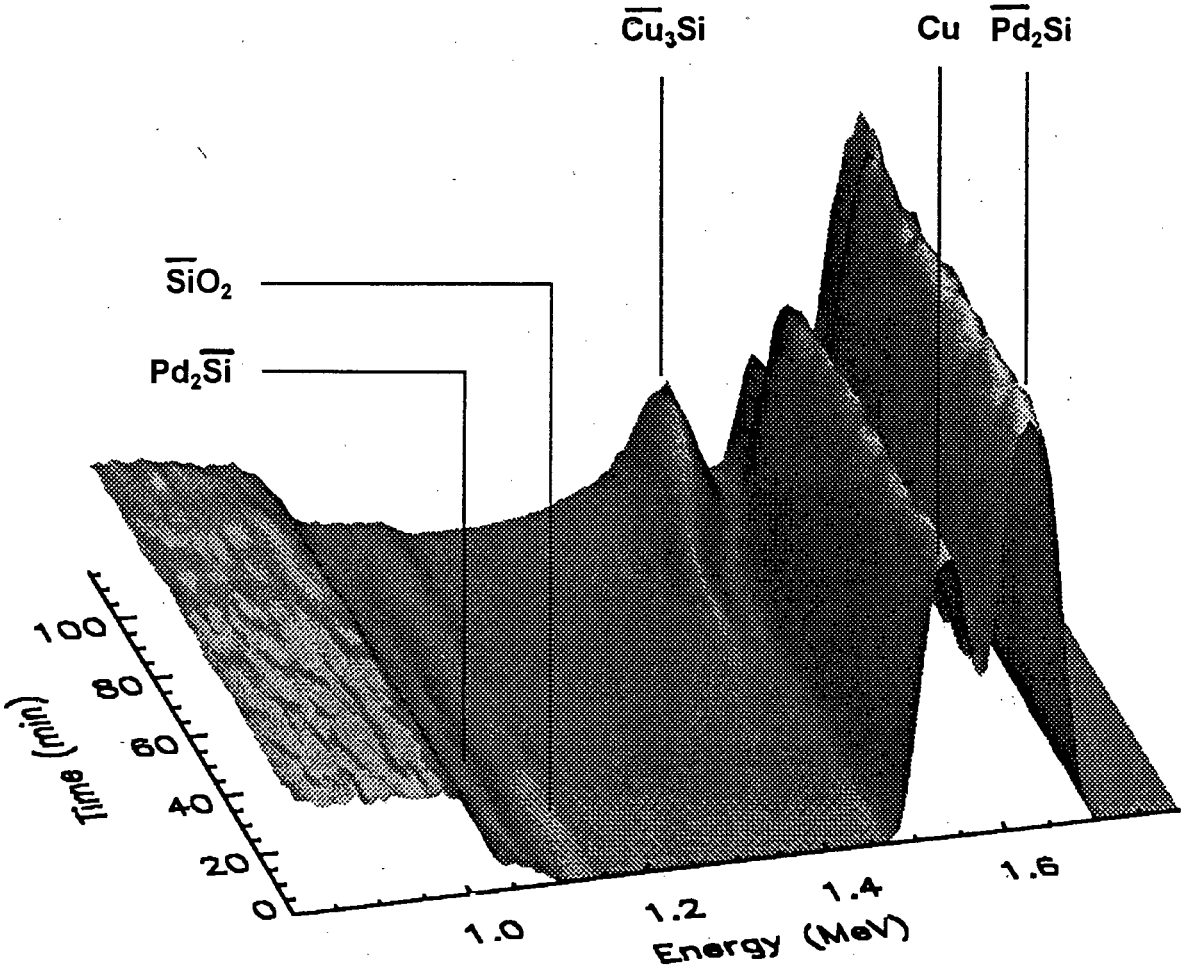

Figure 4-4: *A plot indicating the continuous* **RBS** *spectra as a function of time for the Si<111> substrate. The* **RBS** *spectra were grouped in two minute intervals. The copper diffusion through Pd_2Si is clearly observed. In this case though the copper diffusion appears to begin at a higher temperature, as if the diffusion is impeded.*

influence, is the local thermal heating on a small area (beam spot) due to the beam. To reduce the possibility the influence of thermal heating, a very low beam current was used in conjunction with a large beam diameter. A typical beam current was 28 nA as opposed to approximately 140 nA using conventional **RBS**.

A test was also performed [Th96] to see if any local thermal heating would have any effect on an observed reaction. The comparative test involved observing the reaction rate at two different beam spots on the same sample, one which was undergoing continuous analysis and the other infrequent analysis. There was no discernible difference in the reaction rates at the two sites. It is therefore believed that the local beam heating due to the beam had little or no effect on the reaction.

4.3 Determining the growth mechanism

Determination of the activation energy using this ramp technique requires knowledge of the specific growth mechanism, i.e. reaction-controlled or diffusion-controlled growth. To determine whether the observed growth is reaction-controlled or diffusion-controlled, a constant temperature anneal had to be performed. If the layer thickness, x varies linearly with time, i.e. $x \propto t$, then the reaction is reaction-controlled, whereas layer thickness which obeys a parabolic relationship with time, i.e. $x^2 \propto t$, indicates that the reaction is diffusion-controlled.

A constant temperature anneal was performed at 238°C on the $SiO_2/Cu/Pd_2Si/Si<100>$ system. A plot of the fraction of copper, which is proportional to the thickness x, as a function of time t is shown in Fig. 4.5. Accompanying the plot figure as an inset is the sample temperature as a function of time. The sample temperature was increased in 'steps' until the desired temperature was reached. This was done to ensure that intended annealing temperature was not overshot for extended periods . It is clear from Fig. 4.5 that there is a linear relationship between the fraction of copper that has diffused across the intermediate Pd_2Si layer and time. The amount of copper that has reacted is proportional to the thickness of the layer forming, hence the thickness of the reacting layer is directly proportional to time. This leads to the conclusion that the Cu_3Si growth is reaction-controlled.

The observation that the growth rate is proportional to time, appears to be in direct conflict with the findings of Hong *et al* [Ho91], who observe diffusion-controlled growth of Cu_3Si. However the sample configuration of the present study is quite different. Here the copper reacts with the silicon substrate after diffusion through a Pd_2Si layer of fixed thickness. If the Cu_3Si layer is much thinner than the interposed Pd_2Si layer then the supply of silicon to the growth interface is likely to be determined by the rate at which copper diffuses through the Pd_2Si layer. In addition the rapid growth of Cu_3Si at these low temperatures indicates copper diffusion through Cu_3Si is rapid. It's therefore very reasonable to expect that the rate limiting step in the present study will be the diffusion of copper through the Pd_2Si layer. As this does not increase in thickness during the process, this will result in Cu_3Si growth being linear with time, giving one the mistaken impression that the diffusion is reaction-controlled.

4.4 Experimental procedure

Dynamic **RBS,** as shown, generates a large amount of data from just a single sample or experimental run. However, one might still expect some variation from sample to sample. So if particular care was taken in sample preparation, the factors mentioned in section 3.7 which were possible causes of variations from sample to sample, could be minimized. One of these factors, which is thought to contribute largely to the spurious results obtained by conventional techniques as discussed earlier, is the varying epitaxial quality of the Pd_2Si layer across the lateral dimensions of the sample. It was therefore reasonable to assume that *dynamic* **RBS** applied to samples in close proximity to each other on the substrate heater during evaporation and subsequent annealing could limit or reduce the variation and provide reasonable reproducible experimental data. Samples occupying positions denoted by an X in Fig. 4.6 were used to undergo temperature ramping. The substrate heater, used in the evaporator to preform the Pd_2Si, showed some evidence of a temperature gradient, from the center directly above the heating elements towards the edges of the heater. Growth and epitaxial quality of the intermediate Pd_2Si layer could have been affected by this temperature gradient. Care was therefore taken to use the samples that were in close proximity to each other,

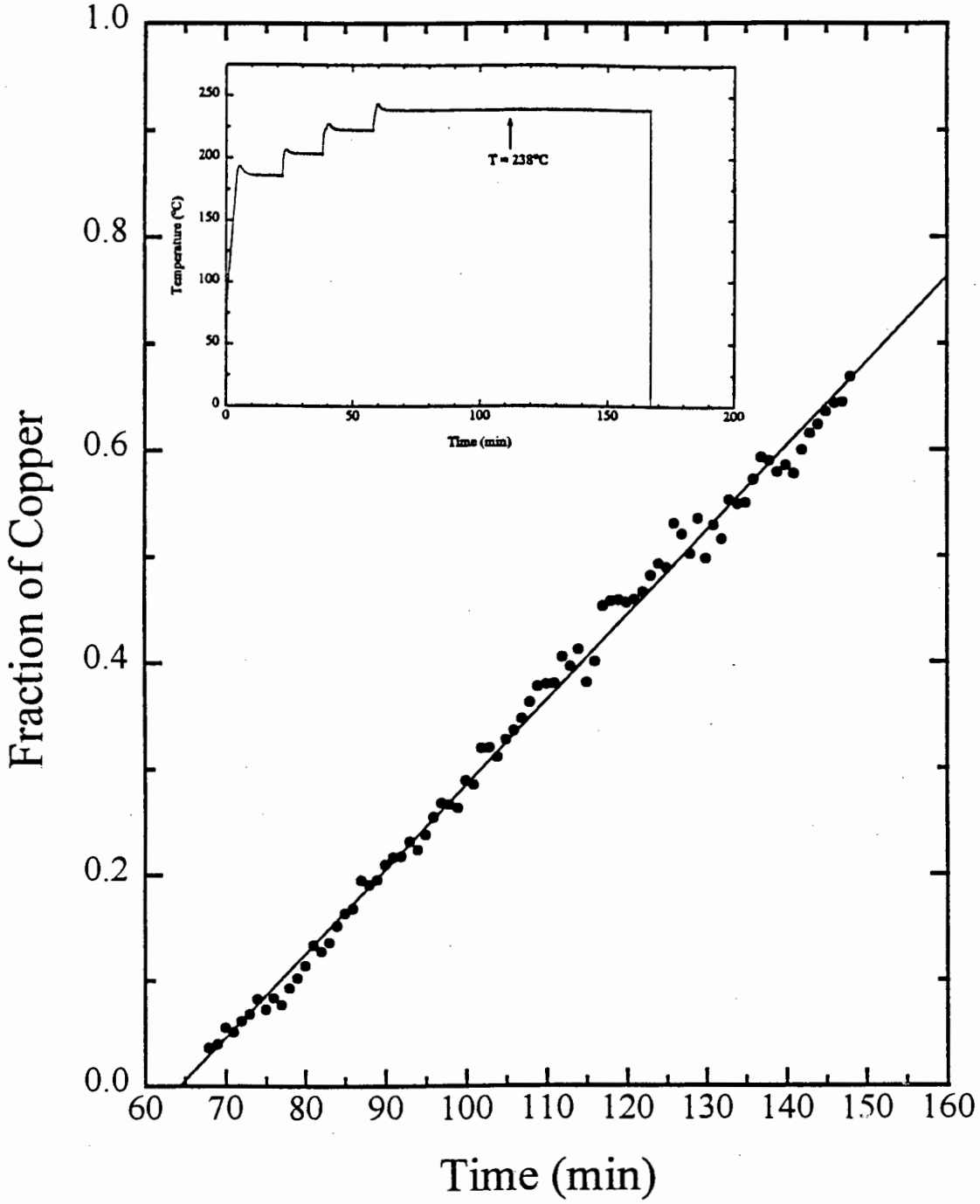

Figure 4-5: *A plot of the fraction of copper that has diffused through the Pd_2Si layer and reacted with the underlying silicon as a function of time at 238° C. The linear relationship indicates reaction-controlled growth. Inset: Variation of sample temperature with time.*

closest to the centre and next to one another. It was hoped that this choice of sampling could considerably enhance the chances of more consistent results.

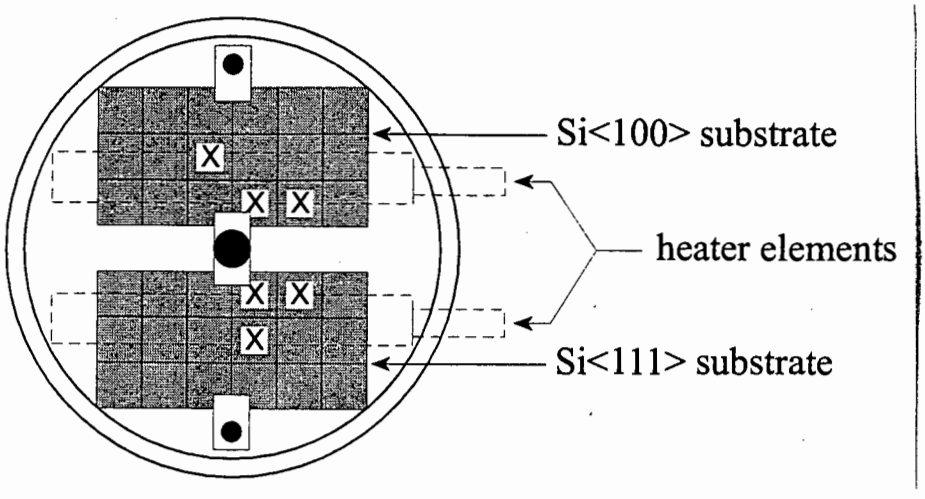

Figure 4-6: *The positions of the samples on the substrate heater prior to loading into the evaporator. The X's represent the samples chosen for analysis and the dashed lines indicate the heater elements.*

4.5 Difference in onset temperatures for diffusion on Si<100> and Si<111> substrates

A total of six samples of the form SiO_2/Cu/Pd_2Si/Si< > underwent *dynamic* **RBS**. Three of the samples were prepared on Si<100> substrates and the other three on Si<111> substrates. After the experimental data was accumulated, **RUMP** analysis was performed to determine the thickness of the Cu-silicide layer. An obvious question that arises now is whether the onset temperature difference between the two different substrate orientations can be observed directly from this data. Indeed it should, if both data sets were plotted on the same set of axes and bearing in mind that any displacement along the inverse temperature axis would indicate a temperature difference. A comparative Kissinger plot for both substrate orientations is shown in Fig. 4.7.

For identically prepared samples undergoing identical heat treatments, one would expect the data for each sample to occupy the same position in the Kissinger plot.

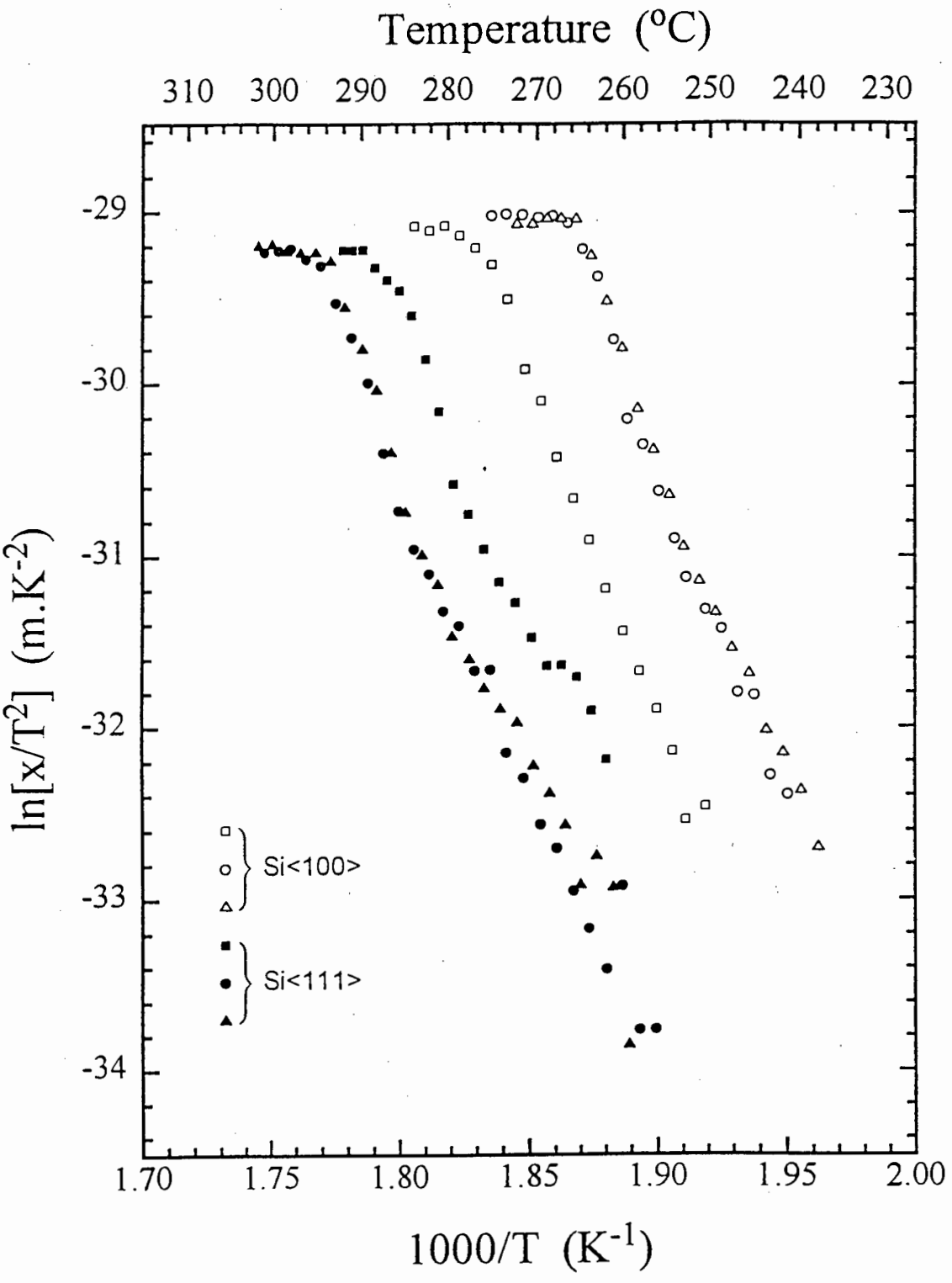

Figure 4-7: *A comparative Kissinger plot. The bottom axis was plotted using the inverse sample temperature. The solid data points indicate Si<111> and the open data points indicate Si<100>. From this there appears to be no temperature difference because the data overlaps.*

However, in both cases one of the samples' data is displaced either to a higher or lower temperature. In the case of Si<100> , it appears that for one of the samples the onset temperature and subsequent silicide formation occurs at a higher temperature than the other two. For Si<111> the opposite is true. Hence, the temperature difference for the onset of copper diffusion was indeterminable due to the overlap. Actually it was thought that this discrepancy was due to the variation in epitaxial quality from sample to sample. However it was noted that the offset in temperature between the sample and oven temperatures varied from one experimental run to another, suggesting that one or both were unreliable. Calibration tests performed by C. Theron [Th96] of the oven and sample temperature readings taken by the thermocouples revealed that the oven temperature was a truer reflection of the absolute temperature during *dynamic* **RBS**, and hence more reliable for the reasons mentioned earlier.

The data was replotted in Fig. 4.8 using the oven temperature instead. In Fig. 4.8 each data set falls on a distinct path, i.e. no observed overlap. Now there is a distinct temperature difference for the two substrate orientations. The difference in temperature for comparable extent of growth on the two slicon substrates is about 20°C over the full duration of the reaction.

4.6 Determination of the activation energy

Now that the growth mechanism is known, the combined Kissinger plot, Fig. 4.8, generated using Eq. (1.16) for reaction-controlled growth as discussed in section 1.2 can be used to determine the activation energy. Again briefly,

$$ln\left(\frac{x}{T^2}\right) = ln\left(K_o \frac{dt}{dT}\frac{k}{\triangle H}\right) - \frac{\triangle H}{kT} \tag{1.16}$$

where x is the thickness of the growing layer, T is the temperature in Kelvin, dt/dT is the inverse ramp rate and $\triangle H$ is the activation energy. A plot of $ln\,(x/T^2)$ as a function of inverse temperature T will therefore yield the activation energy directly from the slope. The inverse temperature T that was plotted was the oven temperature.

Linear regression was performed on the data and the best fit curves generated are

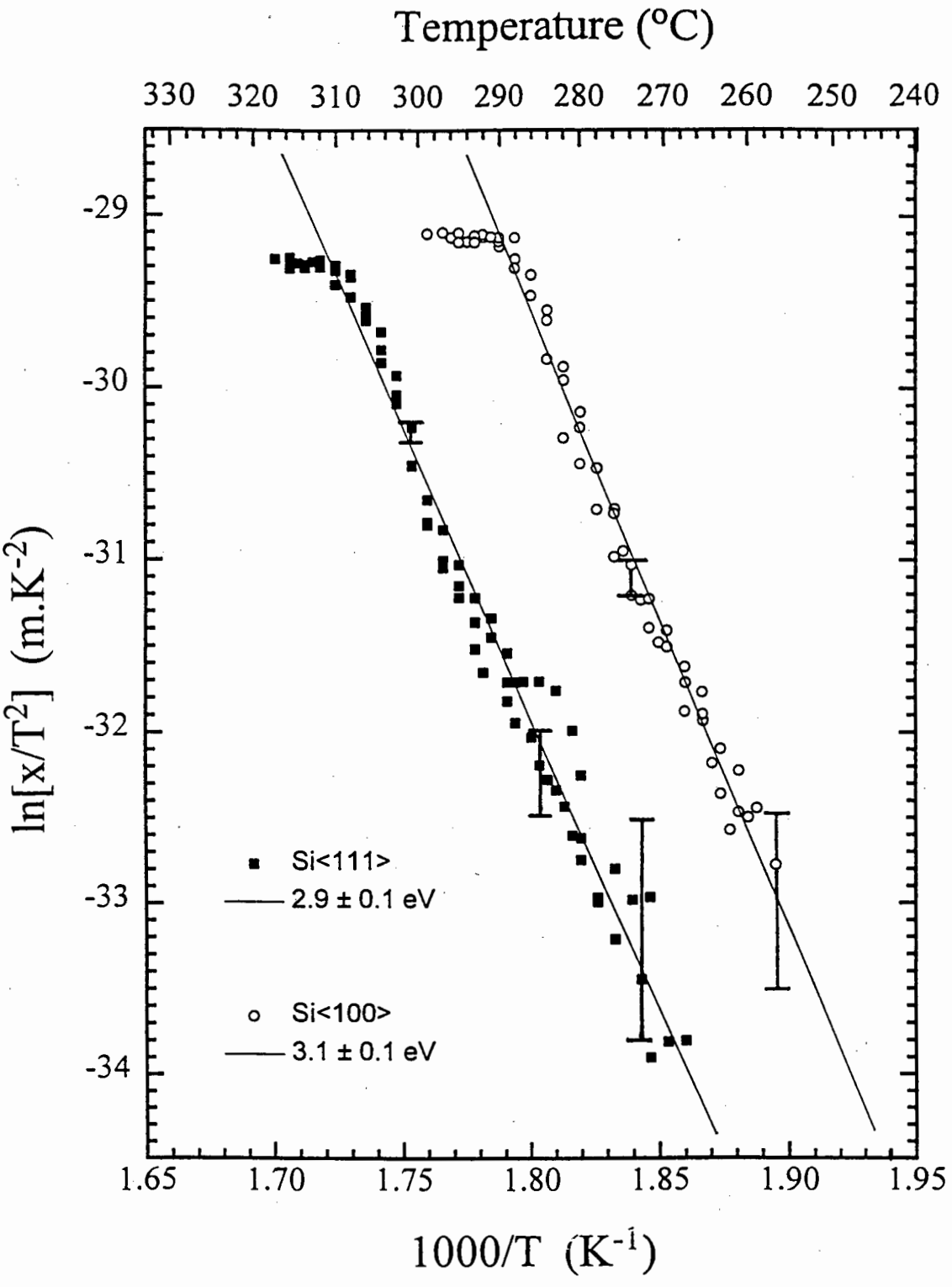

Figure 4-8: *A comparative Kissinger plot. The bottom axis was plotted using the inverse oven temperature. The temperature difference is clearly observed to be of the order of 20° C.*

also shown in Fig. 4.8. A summarized table of the slopes and the determined activation energies is shown in Table 4.1.

Table 4.1: *A comparative table indicating the activation energies for copper diffusion through Pd_2Si grown on two different substrate orientations. The units are eV.*

		Si<100>	Si<111>
activation energy	$\triangle H$	3.1±0.1	2.9±0.1

Because the slopes observed in Fig. 4.8 are almost the same, the activation energies are therefore comparable within experimental error. This being the case, indicates that the diffusion mechanism is the same for diffusion on both substrate orientations.

4.7 Summary

The activation energy was found to be the same (within experimental error) on both silicon substrates. This strongly suggests that the diffusion mechanism is the same on both substrates. Since the earlier investigation showed that the difference in behaviour between the two substrates was a consequence of the epitaxial quality of the Pd_2Si layer grown on the two substrates and also since the diffusion mechanism through the layers is the same there is only one possible explanation. This is that the mechanism is one of grain boundary diffusion in the case of both silicon substrates with the diffusion on Si<111> inhibited by the low angle grain boundaries found in the epitaxial Pd_2Si layer.

Chapter 5

Summary and Conclusion

Metal silicide films have become very important in present day microelectronic technology due to there applications as contacts, interconnects or diffusion barriers. Advances therefore in semiconductor research is of utmost importance in the evolution of device design and manufacturing. Silicides, like Pd_2Si are often used as electrical contacts to silicon and in general have good conductivity. The use of copper as a substitute for aluminium interconnects poses a new set of challenges, one being the high reactivity of copper with silicon at device processing temperatures. This being the case, an investigation of the reaction kinetics of copper with Pd_2Si and silicon could yield a better understanding of copper-silicide or copper-silicon interaction.

In this investigation the interaction of copper with Pd_2Si and with the silicon substrate was studied. Samples with the configuration $SiO_2/Cu/Pd_2Si/Si< >$ were prepared and subjected to thermal anneals in the temperature range 180°C - 300°C. It was found that the copper in the surface layer diffused through the Pd_2Si layer and reacted with silicon at the $Pd_2Si/Si< >$ interface to form Cu-silicides. This copper diffusion took place at relatively low temperatures, around 200°C, with no visible copper interaction with the intermediate Pd_2Si layer as evident from the Pd_2Si layer appearing to retain its overall composition and thickness. The rate of copper diffusion was found to be very temperature dependent.

Upon further investigation of the $SiO_2/Cu/Pd_2Si/Si< >$ system it was found that the onset of copper diffusion through the Pd_2Si layer was influenced by whether the sili-

cide was grown on Si<100> substrates or Si<111> substrates. Great care was taken to ensure preparation of the silicides was as identical as possible but the onset temperature for copper diffusion through Pd_2Si grown on the two different substrate orientations always differed by approximately 20°C. Since a previous investigation reported that the reaction rates for Cu/Si<100> and Cu/Si<111> systems were different, it was speculated that this difference in onset temperature could be due to the rate of Cu-Si interaction at the Pd_2Si/Si< > interface. The rate of copper interaction with the two silicon substrate orientations was reinvestigated but no evidence of the difference in 'growth rates' of the Cu-silicide was observed. It was then concluded that the onset temperature difference could only be attributed to the Pd_2Si microstructure.

The Pd_2Si microstructure was investigated by **RBS** channeling. The channeling data indicated that the as grown Pd_2Si layer had reasonable epitaxial quality with a minimum yield of approximately 55%. Although lower minimum yields for Pd_2Si have been reported in the literature the minimum yield of ~55% is respectable given that the samples were prepared under moderate vacuum and thermal annealing conditions. No change in minimum yield was observed after the copper has diffused across the Pd_2Si layer, indicating that the copper had not been incorporated into the Pd_2Si layer, i.e. the copper does not interact with the Pd_2Si layer. This behaviour is what one might associate with grain boundary diffusion rather than bulk diffusion. This suggested an explanation as to why there was a difference in onset temperature for copper diffusion. Since epitaxial films have lower angle grain boundaries than non-epitaxial films, one should expect to find that grain boundary diffusion is inhibited by these low angle grain boundaries present in epitaxial films. This could explain why the onset temperature for copper diffusion through Pd_2Si grown on Si<111> is higher than for Pd_2Si grown on Si<100>.

To confirm this proposal an attempt was made to measure the activation energy ($\triangle H$) for Cu-silicide growth. Difficulties were however experienced in this regard because of large variations from sample to sample. To overcome these problems the *dynamic* **RBS** technique was employed to investigate the SiO_2/Cu/Pd_2Si/Si< > system. This technique allowed continuous **RBS** monitoring of the sample during annealing, thereby generating a large amount of data from a single sample. To determine the ac-

tivation energy of the copper diffusion reaction, the growth mechanism first needed to be determined. This was done by performing a constant temperature anneal using this technique. A plot of the fraction of Cu-silicide grown as a function of time indicated that the growth rate of the Cu-silicide was proportional to time, i.e. $\propto t$.

Once it had been established that the growth rate was proportional to time the activation energy could be determined by generating Kissinger plots from data collected while the temperature was ramped at 1°C/min. The activation energy determined for Cu-silicide growth on Si<100> was 3.1±0.1 eV and for Cu-silicide growth on Si<111> was 2.9±0.1 eV. The Kissinger plot also provided conclusive proof for the difference in onset temperature for copper diffusion on the two different substrate orientations. A measurement of $\triangle$T, the onset temperature difference, produced a value of the order of 20°C.

To summarize, copper is found to diffuse via grain boundary diffusion through the Pd_2Si layer to form Cu-silicides at the Pd_2Si/Si< > interface. There is a difference in onset temperature of approximately 20°C for copper diffusion through Pd_2Si grown on Si<100> and Pd_2Si grown on Si<111>. It is proposed that the reason for this difference is that the Pd_2Si grows epitaxially on Si<111> and not so on Si<100>. The epitaxial Pd_2Si has lower angle grain boundaries in comparison to Pd_2Si grown on Si<100>. Grain boundary diffusion is inhibited by the low-angle grain boundaries present in the epitaxial Pd_2Si. The activation energies for Cu-silicide growth on Pd_2Si/Si<100> and Pd_2Si/Si<111> were measured to be 3.1±0.1 eV and 2.9±0.1 eV respectively. Because these activation energies for the two systems were very similar it can be concluded that the copper diffusion mechanism is identical for both systems, although inhibited in the case of the Si<111> orientation. These values for activation energy are, however, larger than one would expect for grain boundary diffusion.

The *dynamic* **RBS** technique proved invaluable to this investigation in terms of understanding the reactions at work in the complex SiO_2/Cu/Pd_2Si/Si< > system. The advantages and pure versatility of this technique over conventional **RBS** techniques is impressive. This opens the research into more complex thin film reactions that were previously impractical.

Appendix A

Binary Phase Diagrams

A.1 Pd - Si phase diagram

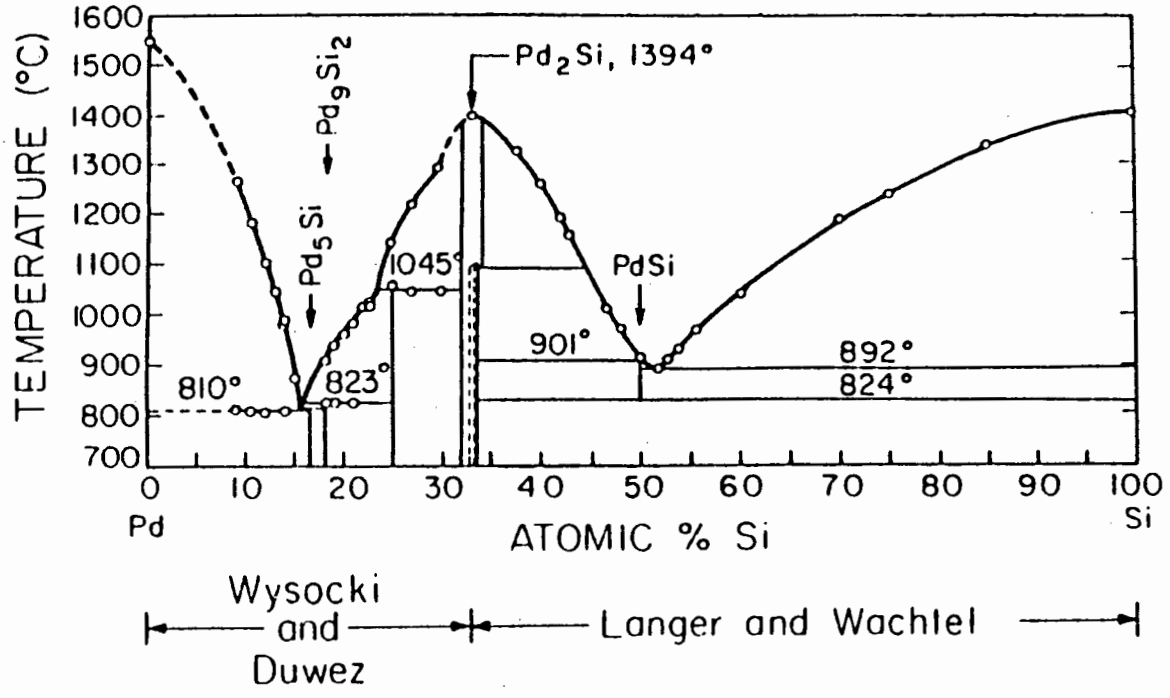

Figure A-1: *Reproduced from Nicolet and Lau [Ni83]. The region $\leq$ 33.3 at.% Si is taken from Wysocki and Duwez [Wy81] and the region $\geq$ 33.3 at.% Si is taken from Langer and Wachtel [La81].*

A.2 Cu - Pd phase diagram

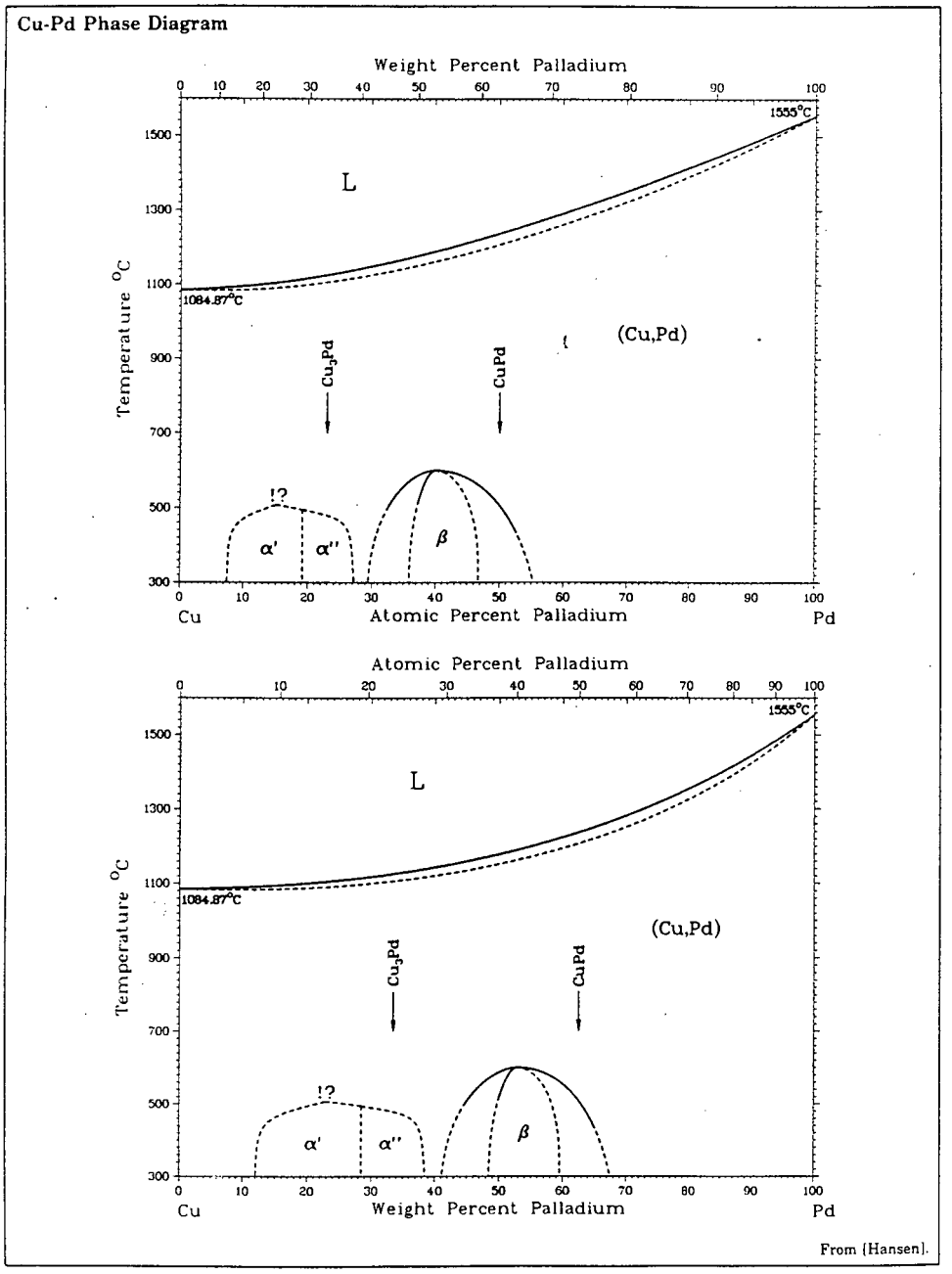

Figure A-2: *Reproduced from Binary Alloy Phase Diagrams [Ma86].*

A.3 Cu - Pt phase diagram

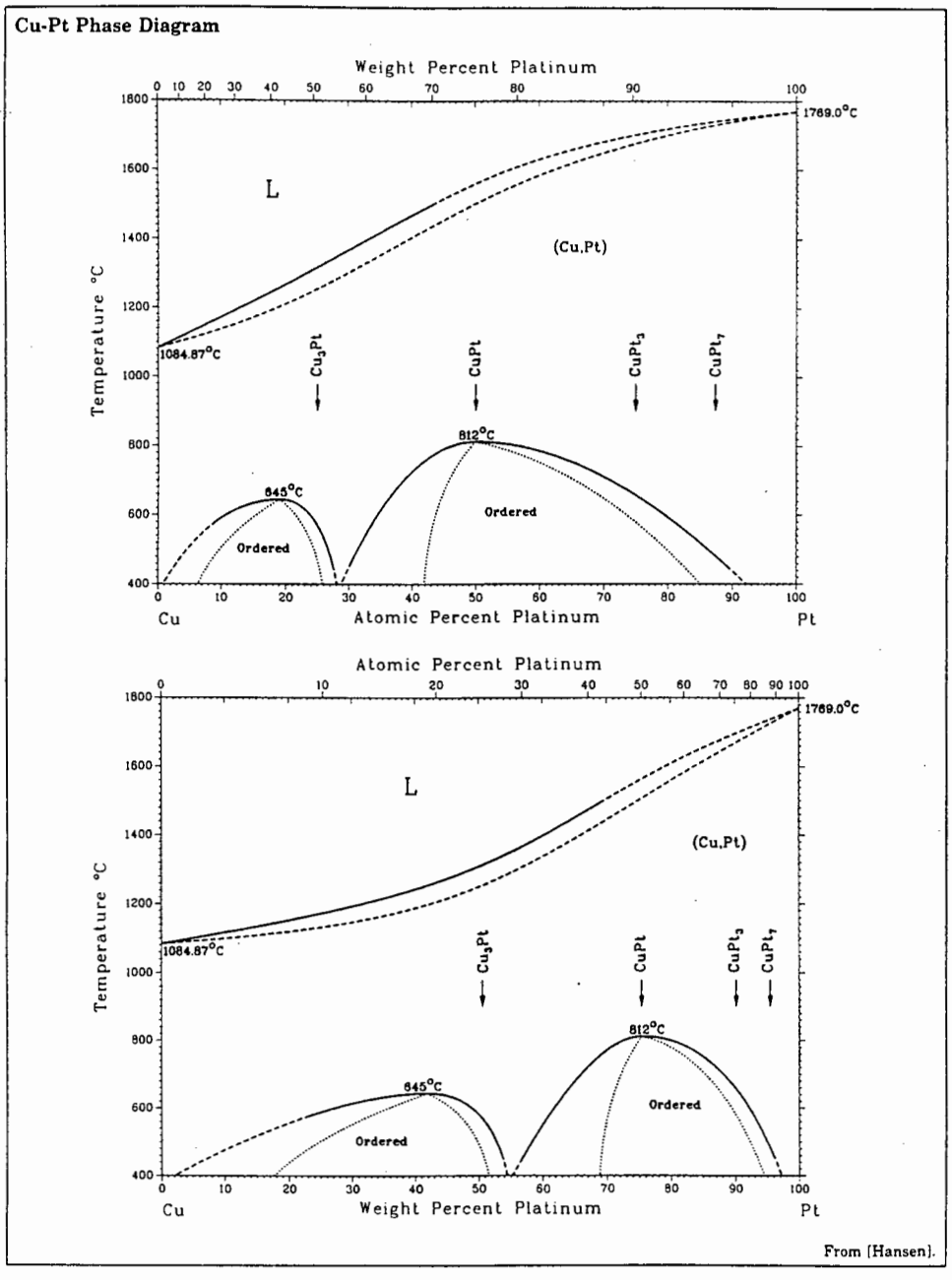

Figure A-3: *Reproduced from Binary Alloy Phase Diagrams [Ma86].*

Bibliography

[Bo88] R.J. Borg and G.J. Dienes, An Introduction to Solid State Diffusion (Academic Press, 1988) 79

[Ch89a] C-A. Chang, Appl. Phys. Lett. **55** (15) (1989) 1543

[Ch89b] C-A. Chang, J. Appl. Phys. **66** (7) (1989) 2989

[Ch90] C-A. Chang, J. Appl. Phys. **67** (1) (1990) 566

[Ch86] L.J. Chen, H.C. Cheng and W.T. Lin, Materials Research Society Symposia Proceedings, eds. R.J. Nemanich, P.S. Ho and S.S. Lau **54** (1986) 245

[Ch78] W.K. Chu, J.W. Mayer and M-A. Nicolet, Backscattering Spectrometry (Academic Press, 1978)

[De65] B.E. Deal and A.S. Grove, J. Appl. Phys. **36** (1965) 3770

[Fe89] D.B. Fenner, D.K. Biegelsen and R.D. Bringans, J. Appl. Phys. **66** (1989) 419

[Fi51] J.C. Fisher, J. Appl. Phys. **22** (1951) 74

[Fu95] M.A. Fury, D.L. Scherber and M.A. Stell, MRS Bulletin **20** (1995) 61

[Ge13] H. Geiger and E. Marsden, Phil. Mag. **25** (1913) 606

[Ge94] A.V. Gelatos, A. Jain, R. Marsh and C.J. Mogab, MRS Bulletin **19** (1994) 49

[Ha94] J.M.E. Harper, E.G. Colgan, C-K. Hu, J.P. Hummel, L.P. Buchwalter and C.E. Uzoh, MRS Bulletin **19** (1994) 23

[Ho91] S.Q. Hong, C.M. Comrie, S.W. Russell and J.W. Mayer, J. Appl. Phys. **70** (7) (1991) 3655

[Ho94] S.Q. Hong, Q.Z. Hong, J. Li and J.W. Mayer, J. Appl. Phys. **75** (1994) 3959

[Is80] H. Ishiwara, Thin Film Interfaces and Interactions eds. J.E.E. Baglin and J.M. Poate (The Electrochemical Society, 1980)

[Ka93] A.E. Kaloyeros and M.A. Fury, MRS Bulletin **18** (1993) 22

[Ka95] I. Kaur, Y. Mishin and W. Gust, Fundamentals of grain and interphase boundary diffusion (John Wiley and Sons, 1995)

[La81] H. Langer and E. Wachtel, Z. Metallk. **72** (1981) 769

[Li93] J. Li, R. Blewer, and J.W. Mayer, MRS Bulletin **18** (1993) 18

[Li94] J. Li, T.E. Seidel, and J.W. Mayer, MRS Bulletin **19** (1994) 15

[Ma86] Binary Alloy Phase Diagrams, eds. T.H. Massalski, J.L. Murray, L.H. Bennett and H.Baker (American Society for Metals, 1986)

[Ma84] H.F. Mataré, J. Appl. Phys. **56** (1984) 2605

[Ma90] J.W. Mayer and S.S. Lau, Electronic Materials Science: for integrated circuits in Si and GaAs (Macmillan, 1990)

[Mi94] N. Misawa, T. Ohba and H. Yagi, MRS Bulletin **19** (1994) 63

[Mu93] S.P. Murarka, J. Steigerwald and R.J. Gutmann, MRS Bulletin **18** (1993) 46

[Ni83] M-A. Nicolet and S.S. Lau, VLSI Electronics: Microstructure Science edited by N. Einspruch (Academic Press, 1983)

[Sh95] L.T. Shi and K.N. Tu, J. Appl. Phys. **77** (1995) 3037

[St95] J.M. Steigerwald, S.P. Murarka, J. Ho, R.J. Gutmann and D.J. Duquett, J. Vac. Sci. Technol. B **13** (6) (1995) 2215

[St91] L. Stolt, F.M.D. Heurle and J.M.E. Harper, Thin Solid Films **200** (1991) 147

[Th94] C.C. Theron, M.Sc. Thesis, University of Stellenbosch 1994 (unpublished)

[Th96] C.C. Theron (1996): Private Communication.

[Th95] C.C. Theron, C.L. Churms, K.A. Springhorn and T. Swart, NAC Annual Report (1995) 45

[Tu78] K.N. Tu and J.W. Mayer, Thin Films - Interdiffusion and Reactions, eds. J.M. Poate, K.N. Tu and J.W. Mayer (John Wiley-Interscience, 1978) p359

[Tu92] K.N. Tu, J.W. Mayer and L.C. Feldman, Electronic Thin Film Science for electrical engineers and material scientists (Macmillan, 1992)

[Tu82] R.T. Tung, J.M. Poate, J.C. Bean, J.M. Gibson and D.C. Jacobson, Proceedings of the Symposium on Thin Films and Interfaces, eds. P.S. Ho and K.N. Tu (North Holland, 1982) p79

[Wh54] R.T.P. Whipple, Phil. Mag. **45** (1954) 1225

[Wy81] J.A. Wysocki and P.E. Duwez, Metall. Trans. **12A** (1981) 1455

[Ya94] J. Yang and H.B. Zhang, Appl. Phys. Lett. **64** (14) (1994) 1800